Diffuse Reflection Infrared Spectroscopy (Drifts): Application to the in Situ Analysis of Catalysts

T. Armaroli, T. Bécue, S. Gautier

Diffuse Reflection Infrared Spectroscopy (DRIFTS): Application to the *in situ* Analysis of Catalysts

T. Armaroli[1], T. Bécue[1] and S. Gautier[1]

1 Institut français du pétrole, IFP-Lyon, BP 3, 69390 Vernaison Cedex - France
e-mail: tiziana.armaroli@ifp.fr - thierry.becue@ifp.fr - serge.gautier@ifp.fr

Résumé — **Spectroscopie infrarouge en réflexion diffuse (DRIFTS) : application à l'analyse *in situ* de catalyseurs** — La technique infrarouge de spectroscopie de réflexion diffuse (DRIFTS), moins pratiquée que la transmission en raison de ses limitations, est extrêmement utile, en effet indispensable, pour les matériaux non transparents et/ou pour des mesures *in situ* à la température élevée. Les auteurs décrivent les principes de cette technique et ses avantages par rapport à la spectroscopie infrarouge en transmission. L'application de DRIFTS à la caractérisation des catalyseurs est illustrée par deux études : sur l'interaction du molybdène avec le précurseur de catalyseurs de désulfuration de carburant, et sur les modifications *in situ* sous gaz réactifs des catalyseurs de réduction des composés azotés dans les gaz d'échappement.

Abstract — *Diffuse Reflection Infrared Spectroscopy (DRIFTS): Application to the* in situ *Analysis of Catalysts* — *The diffuse reflection infrared Fourier transform spectroscopy (DRIFTS) technique, less practiced than the transmission mode because of its limitations, is extremely useful, indeed indispensable, for non-transparent materials and/or for* in situ *measurements at elevated temperature. The authors describe the principles of this technique and its advantages over transmission infrared spectroscopy. The application of DRIFTS to the characterization of catalysts is illustrated by two studies conducted on the interaction of molybdenum with the precursor of fuel desulphurization catalysts, and on the* in situ *modifications under reactive gases of catalysts for reducing nitrogen compounds in exhaust gases.*

INTRODUCTION

Owing to their wide variety of composition and structure, heterogeneous catalysts pose a major challenge to characterization techniques. In recent years, to achieve a detailed description of the structural changes in catalysts under reactive atmosphere, many analytical developments have been carried out in the area of *in situ* analysis. Infrared spectroscopy is an ideal technique that is widely used to characterize the acidity of supports and deposited metallic phases. This technique is currently limited to the analysis of samples transparent to IR radiation and formed into the shape of a self-supported pellet. Some samples cannot be analyzed due to the lack of mechanical strength and/or transmission. This applies in particular to hydrated samples or certain catalysts used to combat automotive pollution. The use of a diffuse reflection accessory and the associated DRIFTS (Diffuse Reflectance Infrared Fourier Transform Spectroscopy) technique helps to circumvent these obstacles and to analyze materials under reactive atmosphere.

1 THEORETICAL REVIEW: DIFFUSE REFLECTANCE INFRARED FOURIER TRANSFORM SPECTROSCOPY (DRIFTS)

Any radiation focused on a surface can, depending on the characteristics of the surface and its environment, be absorbed, directly reflected (specular reflection), internally reflected, or diffused in all directions. The latter effect is of interest in diffuse reflection spectroscopy [1]. One of the principal advantages of this technique is the ability to obtain infrared spectra of solid materials without cumbersome sample preparation. However, DRIFT spectra may be extremely difficult to interpret because they closely depend on the conditions in which they are obtained.

As shown in Figure 1, infrared radiation may be directly reflected by the sample surface, giving rise to specular refraction, which is a function of the refractive index and absorbtivity of the sample. The radiation may also undergo multiple reflections occurring at the surface of the particles and without penetrating the sample.

The radiation that undergoes this type of diffuse specular reflection exits the surface at any angle relative to that of the incident beam. On the contrary, true diffuse reflection is the consequence of beam penetration into one or more particles and its diffusion in the sample. This component of the radiation also exits the sample at any angle but, since it has traveled through the particles, it contains data on the absorption properties of the material. In consequence, this complex radiation contains similar data to those of a transmission spectrum, and this is why it is advantageous from the infrared spectroscopy standpoint. However, diffuse reflection cannot be optically separated from specular
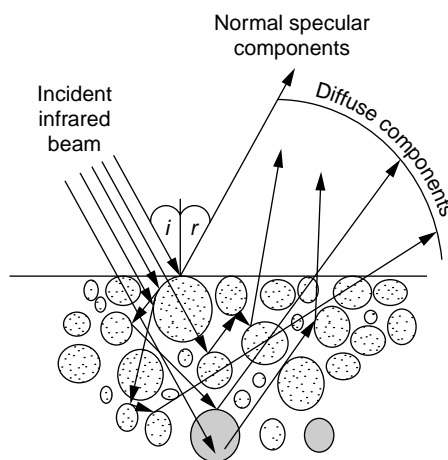

Figure 1

Mechanisms generating the infrared spectrum of a powder.

reflection, but if the specular diffuse reflection component is weak compared with diffuse reflection (absorptivity of the material not too high), diffuse reflection spectra are very similar to transmission spectra. The contribution of specular reflection to the total signal is the main cause of the distortion of DRIFT spectra.

As a rule, the specific properties of the material liable to influence the quality of the DRIFT spectrum are as follows:
- refractive index of the sample;
- particle dimensions;
- packing density;
- homogeneity;
- concentration;
- absorption coefficients.

In the case of inorganic or strongly absorbent materials, the first three properties can cause significant distortions in the form and relative intensity of the bands, to the extent of having negative bands. To decrease the contribution due to external reflection of the largest particles, the sample can be ground into smaller particles. A size smaller than 10 μm (*i.e.* not exceeding the wavelength of the incident radiation) is preferable. If the sample is too absorbent, it must be diluted in a nonabsorbent matrix (potassium chloride, KCl or potassium bromide, KBr). In general, dilution guarantees deeper penetration of the incident ray and less specular reflection of the sample surface, thereby increasing the contribution to the spectrum of components which contain data on the absorbance properties. In certain cases, however, as for zeolites, this type of matrix cannot be used because of interactions with the sample. If so, the use of pure zeolite powder is indispensable.

From the theoretical standpoint, there is no linear relation between band intensity and concentration, and quantitative analyses by the DRIFTS method are rather complicated.

The Lambert-Beer law, normally used in transmission, is not directly applicable. However, a similar expression can be found by applying the Kubelka-Munk equation. Let us consider a given sample, of thickness d, subject to an incident flux I_0 in direction x and which reflects a flux J_0 along the same axis but in the opposite direction *(Fig. 2)*. In the element of thickness dx, the fraction of light transmitted is proportional to k (absorption coefficient) and the fraction of light diffused is proportional to parameter s (diffusion factor).
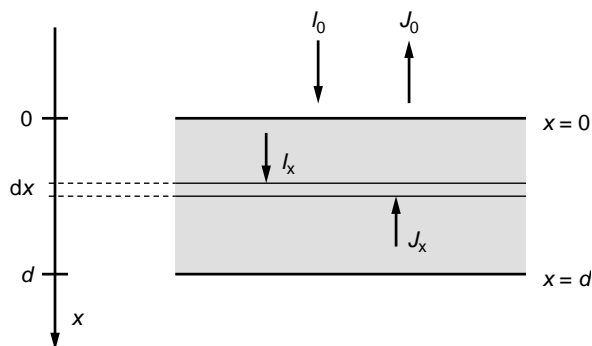

Figure 2

Schematic representation of a layer of particles which absorb and diffuse light.

Using this simple model, we can show that the transmittance (ratio of the intensity of the exiting light to the entering light crossing the sample) can be expressed by:

$$T = \frac{I_{x=d}}{I_0} = \frac{2\beta}{(1+\beta^2)\sin h(k'd) + 2\beta\cos h(k'd)}$$

and diffuse reflection:

$$R = \frac{J_{x=0}}{I_0} = \frac{(1 - \beta^2\sin h(k'd)}{(1+\beta^2)\sin h(k'd) + 2\beta\cos h(k'd)}$$

in these expressions:

$$k' = |k(k+2s)|^{1/2} \qquad \beta = |\frac{k}{h+2s}|^{1/2}$$

While k, the absorption coefficient, is easily known from the Lambert-Beer law, parameter s is difficult to determine. To circumvent this problem, Kubelka and Munk [2] considered the limiting case of a sample of infinite thickness (2 or 3 mm of powder satisfies this condition). This accordingly gives:

$$T_\infty = 0 \qquad \text{and} \qquad R_\infty = (1-\beta)/(1+\beta)$$

which can also be placed in the form:

$$\frac{(1 - R_\infty)^2}{2R_\infty} = \frac{k}{s} = f(R_\infty)$$

$f(R_\infty)$ is called the re-emission function or Kubelka-Munk function. A comparison with a standard sample consisting of a very nonabsorbent powder, *i.e.* KCl, KBr, etc. (such that $k \cong 0$ and $R_\infty \cong 1$) helps to determine the ratio:

$$r_\infty = (R_\infty) \text{ sample } / (R_\infty) \text{ standard}$$

to which we apply the expression:

$$f(r_\infty) = (1 - R_\infty)^2 / 2 R_\infty = k/s$$

by replacing k by $2.303*\varepsilon*c$, where:

ε = extinction coefficient (function of the wavenumber ν);

c = sample concentration;

this gives:

$$f(r_\infty) = 2.303*\varepsilon(\nu)*c/s$$

and if s is a constant, *i.e.* an intrinsic property of the material which depends on the grain size, $f(r_\infty)$, at a given frequency, varies directly with the sample concentration c. This produces a similar expression to the absorbance expression that enables us to obtain a spectrum resembling the transmission spectrum.

Diffuse reflection measurements are mostly limited to semi-quantitative analyses. This technique is extremely useful for examining samples that are difficult to analyze in transmission.

2 DRIFTS APPARATUS

Figure 3 shows the apparatus for the DRIFTS measurement. The infrared beam is focused by a series of mirrors on the surface of the sample, which is placed in a sample holder. Diffuse radiation through the powder is collected by other mirrors and sent to the detector.
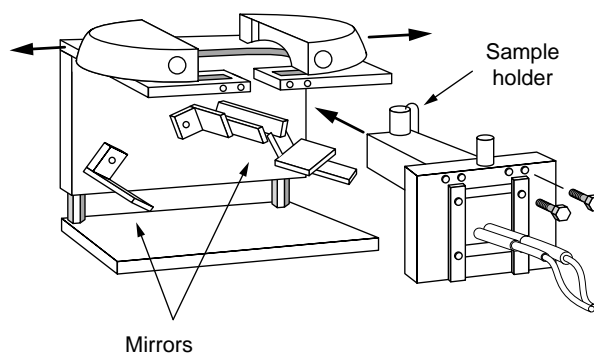

Figure 3

Apparatus for diffuse reflection measurements.

The apparatus can be equipped with an *in situ* high temperature and high pressure cell shown in Figure 4. The sample holder, a ceramic crucible containing a heating resistor and a thermocouple, is placed inside a dome with zinc selenium (SeZn) windows that can withstand a maximum temperature of 473 K (200°C). To remove the heat, the dome is surrounded by coils conveying a stream of nitrogen gas kept at low temperature by a heat exchanger immersed in liquid nitrogen. To prevent condensation on the windows, the liquid nitrogen flowrate must be regulated as a function of the final sample temperature.

An inlet and outlet are provided to send the gases into the dome and through the sample.

Figure 5 shows the path of the gases inside the dome. The gases pass through the sample from the bottom upward. This flow direction offers the advantage of thermostatically controlling the gases and tracking the surface reactions at the desired temperatures.

This *in situ* cell serves to:

– subject the sample to reactive conditions simulated by the sending of different gaseous mixtures;
– reach a temperature of 1173 K (900°C) at atmospheric pressure or 673 K (400°C) at 1500 psi (100 bar);
– record the sample spectra at elevated temperatures;
– directly measure the sample temperature by a thermo-couple in intimate contact with the powder *(Fig. 5)*.

3 CHARACTERISTICS OF THIS TECHNIQUE: ADVANTAGES AND DRAWBACKS

The DRIFTS technique offers the advantages of simpler sample preparation, the capacity to analyze nontransparent samples, irregular surfaces and coatings (polymer, etc.), exposure of the sample to simulated reaction conditions while analyzing the changes in the species at the material surface, recording of the spectrum of the powder at elevated temperature and/or under pressure. The main drawback is the difficulty of quantitative measurements. Another limitation concerns the repetitivity of the measurements. Since the diffusion coefficient varies with each preparation, it is difficult to compare two spectra of the same material recorded in two different experiments [3]. To overcome this problem, the spectra can be brought to iso-intensity of a structure band. In the case of boehmites, for example, the spectra were set to scale by equalizing the band intensities around 2090 and 1970 cm^{-1}, bands due to the harmonics of the bands of the boehmite structure. Thus the differences between the samples can be appreciated by analyzing the variations in relative band intensities (see Section on boehmites below). Other drawbacks concern the implementation of the diffuse reflection experiment to analyze catalysts. A high temperature gradient exists between the upper edge and bottom of the crucible containing the sample. The infrared radiation cannot see the entire thickness of the catalytic bed but only the sample surface. In consequence, differences may be recorded between the reactivity observed by the changes in the bands of the species at the surface and that obtained by analyzing the gases exiting the cell. This is why, in our case, surface analysis is insufficient to track the reaction, and the gases leaving the DRIFTS cell must be analyzed, either by infrared analysis or by mass spectrometry. The recording temperature also affects the position, width and intensity of the bands of a spectrum (see Section 5.1 on hydroxyls of zeolite Y). In order to compare the samples, it is therefore necessary for the spectra to be recorded at the same temperature.
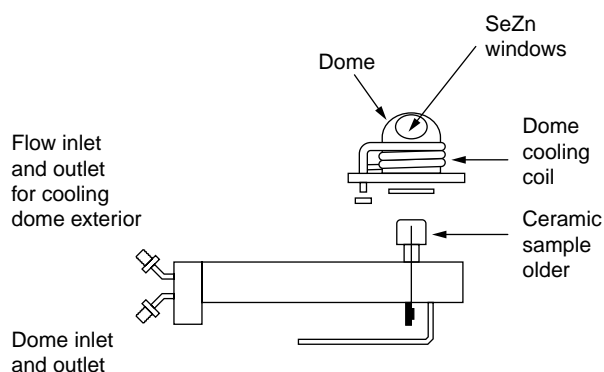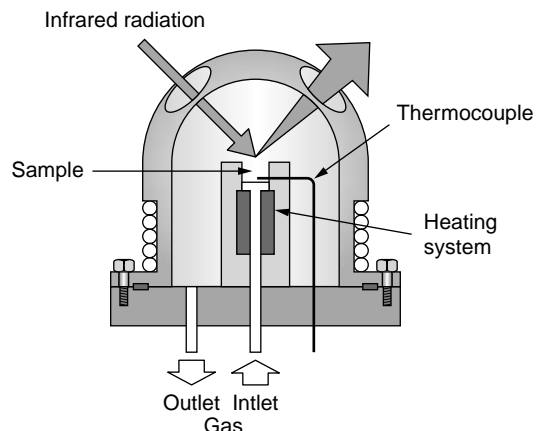

Figure 4

Sample holder and dome.

Figure 5

Dome interior.

4 COMPARISON OF DRIFTS WITH TRANSMISSION IR SPECTROSCOPY

To compare IR spectroscopy in DRIFTS and transmission mode, let us consider the spectrum of an organic substance recorded in the simplest conditions, *i.e.* at ambient temperature and with nitrogen blanket inside the instrument. The compound 1,2-bis(diphenyl phosphino)ethane was selected, because it displays several characteristic bands around 3000 cm^{-1} and below 2000 cm^{-1}. The reference spectrum (background) employed in this case was acquired with a mirror at ambient temperature and under nitrogen. The diffuse reflection spectrum of 1,2-bis(diphenyl phosphino)ethane at 298 K is shown in Figure 6. The bands are clearly identified, with a "correct" baseline and a highly favorable signal-to-noise ratio.
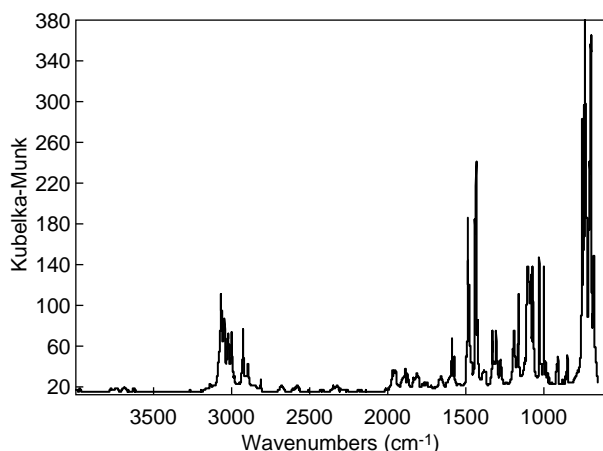

Figure 6

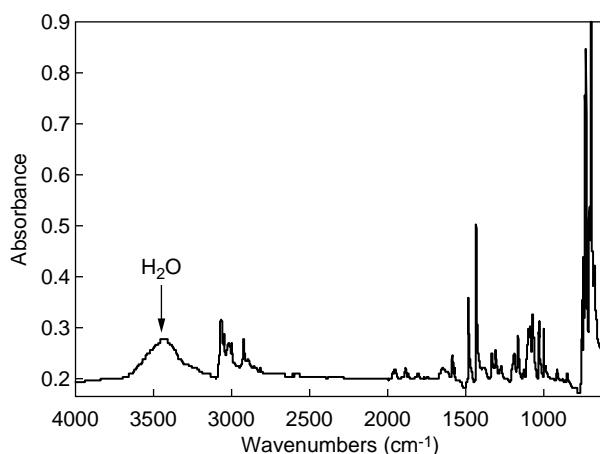DRIFT spectrum of 1,2-bis(diphenyl phosphino)ethane, pure powder, at 298 K.

Figure 7

Transmission spectrum of 1,2-bis(diphenyl phosphino)ethane, KBr pellet, at 298 K.

The diffuse reflection infrared spectrum can be compared with that of the same substance recorded in transmission *(Fig. 7)*. In this case the sample is a 300 mg pellet of potassium bromide (KBr) containing a few milligrams of 1,2-bis(diphenyl phosphino)ethane and the spectrum is recorded in the same temperature and atmospheric conditions used in diffuse reflection. Both spectra are virtually equivalent and furnish the same data on the substance concerning the number of bands, relative intensity and peak positions. In case of transmission analysis, a wide and intense band is found below 3500 cm^{-1} due to the water present in the KBr of the pellet.

To conclude, in this specific case, the diffuse reflection technique combines the advantage of faster and simpler sample preparation with the absence of the spurious water band in the spectrum.

5 APPLICATION OF DRIFTS AT VARIABLE TEMPERATURES

Let us now consider the case of a variation in the temperature of a sample flushed with a constant gas flowrate.

The heating system is used to control the temperature ramp-ups, to produce plateaux and to implement heating and cooling cycles. The decomposition of calcium oxalate (CaC_2O_4), routinely used as a reference in thermogravimetric analysis (TGA), illustrates the data that can be obtained. The TGA operating procedure comprises the following parameters:

– about 14 mg of sample (pure powder);
– an inert gas flowrate of 4 l/h (or ~ 66.6 ml/min);
– heating from 293 to 1073 K, 10 K/min.

Analysis by thermobalance reveals three endothermic conversions due respectively to:

– departure of water at ~ 435 K;
– conversion of oxalate to carbonate at ~764 K ($CaC_2O_4 \rightarrow CaCO_3 + CO$);
– conversion of carbonate to Ca oxide at ~993 K ($CaCO_3 \rightarrow CaO + CO_2$).

For the DRIFTS analysis, the temperature rise was set at 10 K/min (from 298 to 1073 K) and the nitrogen flowrate at 4 l/h. Spectra of the sample surface were recorded continuously during heating (100 scans, resolution 2 cm^{-1}, about 30 spectra/h). The reference *background* for the entire series was the KBr powder spectrum recorded in a single beam under nitrogen at 373 K. To prevent the saturation of certain signals, the oxalate was diluted in a proportion of 5/95 by weight with ground and dried KBr. The conversions found in thermogravimetry are observed. Around 415 K, the bands above 3000 cm^{-1} virtually disappear and this is associated with the departure of water at 435 K in thermogravimetry *(Fig. 8)*. Above this temperature, the spectra nearly all remain identical up to 739 K except for the formation of a fine,
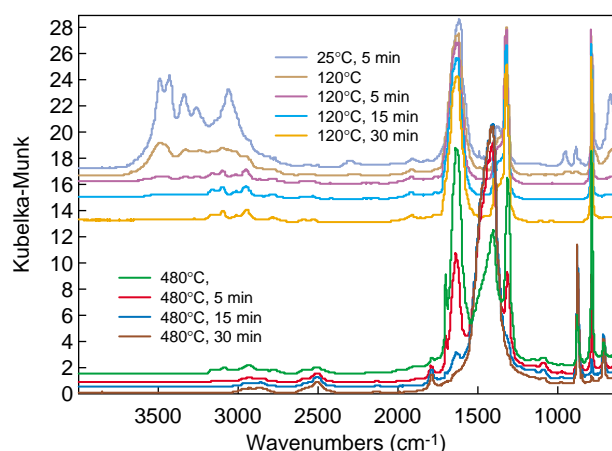
Figure 8

DRIFT spectra of Ca oxalate + KBr (5/95 w/w) et room temperature (common scale).

medium-intensity band around 1698 cm^{-1}. Observable between 739 and 759 K is the progressive decrease, up to complete disappearance, of the bands at 1698, 1636, 1316 and 786 cm^{-1}, simultaneously with the formation of three bands: an intense and wide band at 1404 cm^{-1} and two fine bands, a first intense band at 875 cm^{-1} and a second of medium intensity at 712 cm^{-1}. These three bands, according to the spectra reported in the literature [4], are attributed to the typical bands of calcite ($CaCO_3$). Diffuse reflection analysis reveals the complete conversion of the oxalate to carbonate at about 760 K, whereas this occurs at 764 K in TGA. We can therefore conclude on a good agreement between the TGA and DRIFTS analyses concerning the temperatures observed relative to the departure of water and the conversion of oxalate to carbonate.

5.1 Effect of Temperature on Analytical Accuracy: Example of the Analysis of OH of Zeolite Y

Under inert atmosphere at variable temperature, two Y zeolites with different Si/Al ratios were analyzed. Figures 9a and 9b show the spectra of Y14 zeolite (with Si/Al ratio of 13.6) in the OH vibration zone. Figure 9a shows the transmission spectrum of the self-supported pure powder pellet after overnight activation under vacuum at 723 K (spectrum recorded under vacuum at 298 K). The typical bands of this zeolite are observed, already amply described in the literature [5-7]. The fine and intense band at 3741 cm^{-1} is due to the free terminal silanols and the band at 3630 and 3566 cm^{-1} to the bridged Al-OH-Si acid hydroxyls located respectively in the supercages and hexagonal prisms. A fairly weak signal at 3670 cm^{-1} can be distinguished, attributable to Al-OH of extra-lattice species, as well as two shoulders at 3552 and 3526 cm^{-1}. The baseline shows a slope resulting

from the size of the particles and generating diffusion mechanisms. Figure 9b shows the diffuse reflection spectrum of the same zeolite at 298 K, after activation for 10 h under nitrogen stream at 723 K. The same bands are found as in transmission [8]. Compared with the transmission spectrum, the DRIFT spectrum exhibits a better baseline. Moreover, the weak band at 3670 cm^{-1} due to the extra-lattice species and the two shoulders at the lowest wavenumbers are much more clearly visible.
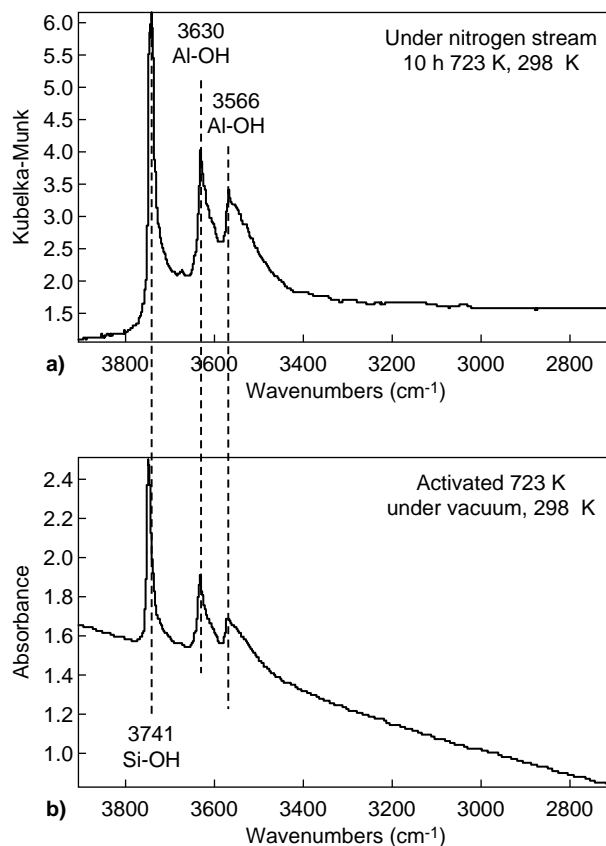

Figure 9

Zeolite Y14 (Si/Al of 13.6). a) transmission spectrum, self-supported pure powder pellet, after overnight activation at 723 K under vacuum; b) diffuse reflection spectrum after 10 h activation under nitrogen. Spectra recorded at 298 K.

We have so far presented zeolite spectra at ambient temperature, but one of the advantages of DRIFTS is the ability to record spectra at variable temperature (*in situ* measurements). Figure 10 shows the DRIFT spectra of zeolite Y14 activated at 723 K and recorded at 723 and 298 K. Note that the temperature has a nonnegligible effect on the spectrum. Comparison of the two spectra, in the case of the spectrum at 723 K *(Fig. 10, a)*, shows that the bands are broader and weaker, the resolution of the shoulders and
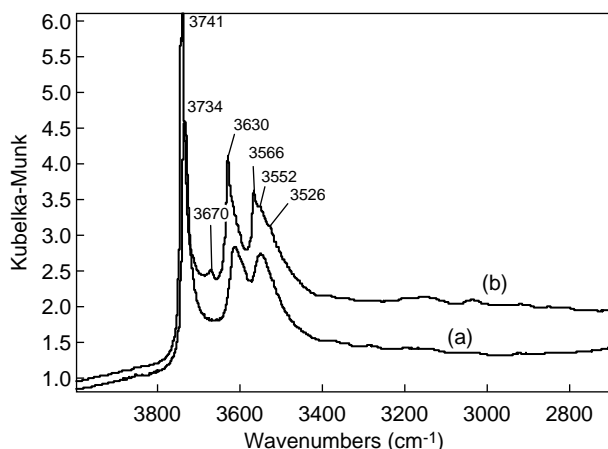
Figure 10

Zeolite Y14 (Si/Al = 13.6) DRIFT spectra under nitrogen after activation (10 h at 723 K), a) at 723 K, and b) lowering to 298 K. Spectra in common scale.
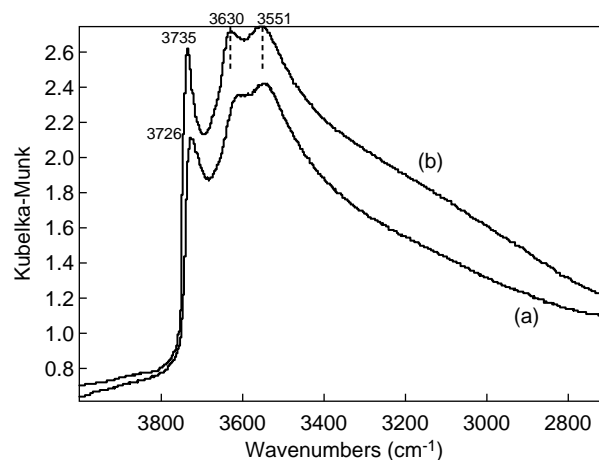

Figure 11

Zeolite Y3 (Si/Al = 2.6) DRIFT spectra under nitrogen after activation (20 h at 723 K), a) at 723 K, and b) lowering to 303 K. Spectra in common scale.

bands is lost, and all the bands are shifted in wavenumber. These effects are due to the diffusion of the infrared beam on the sample, which decreases with rising temperature. The signal-to-noise ratio accordingly decreases.

Another zeolite, Y3 with Si/Al ratio of 2.6, was also analyzed. The DRIFT spectra recorded at high temperature and ambient temperature after activation at 723 K are shown in Figure 11. This shows the band of the free terminal silanols at 3735 cm^{-1} and those of the acid hydroxyls at 3630 and 3551 cm^{-1}. The latter two bands are broader and more intense than those of zeolite Y with a higher Si/Al ratio. In consequence, the effects of temperature on the bandwidths are less pronounced. Note that once the temperature of the sample falls from 723 to 303 K under nitrogen, the zeolite adsorbs a part of the water present in traces in the gas stream. Two bands appear, a very wide band at 3200 cm^{-1} due to the hydroxyls interacting with the water, and a second around 1630 cm^{-1} corresponding to the water deformation modes.

5.2 Location of Molybdenum in Mo/Boehmite Systems and Conversion to γ Alumina

Continuing the study of different materials at variable temperature and under inert atmosphere, the case of boehmites was then considered.

Structure of Boehmite

Crystalline boehmite (chemical formula AlOOH) is an orthorhombic material with a lamellar structure. It consists of a double chain (AlOOH) (infinite) in the *a* direction and perpendicular to the *b* axis *(Fig. 12)*. The aluminum atoms are

located in distorted $AlO_4(OH)_2$ octahedral sites. The hydroxyl groups are at the surface of the layers. Structural cohesion is provided by the hydrogen bonds between the hydrogen atoms of the hydroxyls belonging to one layer and the oxygen atoms of the hydroxyls belonging to the neighboring layer. By heating above 750 K the boehmite is converted to γ alumina. The mechanism generally proposed for boehmite decomposition is based on the elimination of water molecules resulting from condensation of the hydrogen atoms and hydroxyl groups between the layers, causing the collapse of the lamellar structure and the formation of γ-Al_2O_3. Each boehmite monocrystal is converted into a particle of γ alumina, preserving its general form in agreement with the topotactic nature of this transformation [3, 9].
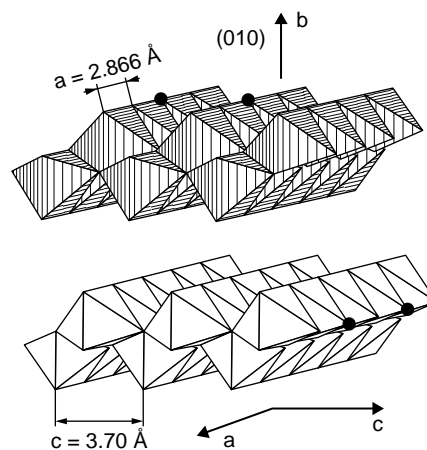

Figure 12

Structure of boehmite (ALOOH formula).

To investigate a new method for synthesizing Mo/Al_2O_3 we examined [10] Mo/boehmite systems and conversions to Mo-alumina. To understand the influence of the metal on the catalytic activity of the final material, it is important to analyze the type of interaction occurring between the molybdenum and the support (boehmite). As already said, the lamellar structure of boehmite consists of a double chain of 2D octahedra with common edges. The compactly of the structure is assured by hydrogen bonds between the hydroxyls of the different planes [11]. The exposed faces are basal and lateral faces. Strongly basic sites are present on plane (101) while face (100) displays weakly basic sites and basal plane (010) is nearly inert *(Fig. 12)* [12]. Raybaud *et al.* [13], according to *ab initio* calculations, proposed four stretching frequencies, corresponding to as many hydroxyl types. The hydroxyls whose stretching frequencies are predicted at 3819, 3741 and 3712 cm^{-1} should be exposed on the lateral planes, respectively (101), (001) and (100). A band anticipated at 3676 cm^{-1} corresponds to the stretching vibration of the neutral OH position of the basal faces *(Fig. 12)*. Morterra *et al.* reported transmission IR spectra of a sample of boehmite activated at 423 K in the form of a thin layer and revealed a rather intense and fine band at 3668 cm^{-1} in the same wavenumber zone and a slight shoulder around 3705 cm^{-1} [14]. They attributed the first to the OH groups of the surface which are released from the hydrogen bond after activation. At lower wavenumber, the two intense and wide bands due to asymmetrical and symmetrical stretching vibrations of the bulk hydroxyls can be recognized at about 3290 and 3090 cm^{-1}. Nonetheless, the interaction of Mo with the OH of the boehmite surface, as well as the conversion of the Mo/boehmite to alumina, has not yet been fully investigated. On the contrary, many studies by infrared spectroscopy are dedicated to calcinated Mo/Al_2O_3 systems

[15-19]. It emerges from these studies that Mo interacts with the hydroxyl groups on the surface of the alumina to form structures of the monolayer type. It has also been shown that at lower Mo content, a preferential interaction appears to occur between the metal and the most basic hydroxyl species [9]. In this context, Mo-boehmite interactions were investigated at increasing Mo content, followed by the conversion of Mo/boehmite to Mo/alumina by the temperature effect. The advantage of DRIFTS mode is illustrated here by comparison with a transmission study of samples in the form of self-supported 20 mg pellets. Figure 13 shows the spectrum of the pure boehmite powder pellet after pretreatment overnight at ambient temperature under secondary vacuum. This type of approach does not allow visualization of the structural hydroxyl vibration bands located at 3340 cm^{-1} and 3125 cm^{-1} owing to saturation of the signal. At higher frequency the band at 3670 cm^{-1} and the shoulders at 3700 cm^{-1} and 3735 cm^{-1}, characteristic of the hydroxyls located respectively on the basal and lateral faces of the boehmite plates, then appear.

Figure 14 shows the spectrum of the same sample of boehmite recorded in diffuse reflection after one night under nitrogen at 298 K. The spectrum is of better quality and does not display any of the band saturation observed in transmission. The infrared spectra presented were recorded with a resolution of 4 cm^{-1} using a mirror as a background reference. For each boehmite sample, a quantity of about 20-25 mg of pure powder was placed in the DRIFTS cell and pretreated at 298 K overnight under nitrogen stream. After taking a spectrum of the sample pretreated at 298 K, the temperature was raised at a rate of 10 K min^{-1} to 873 K with a series of plateaux of 10 to 45 min at fixed temperatures (353, 473, 573 and 723 K). A spectrum was recorded at the end of each plateau. All these tests were conducted under nitrogen.
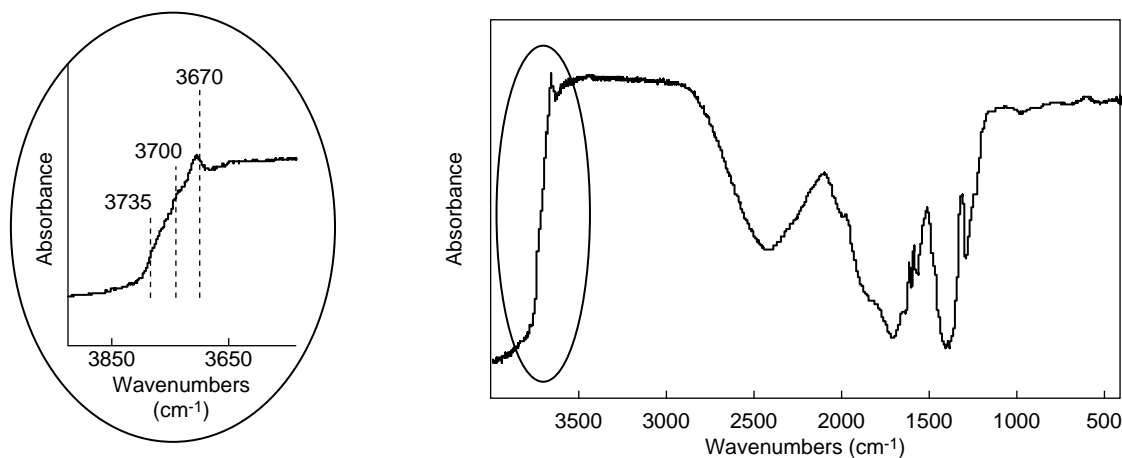

Figure 13

FT-IR spectrum of pure boehmite after one night under secondary vacuum at ambient temperature.
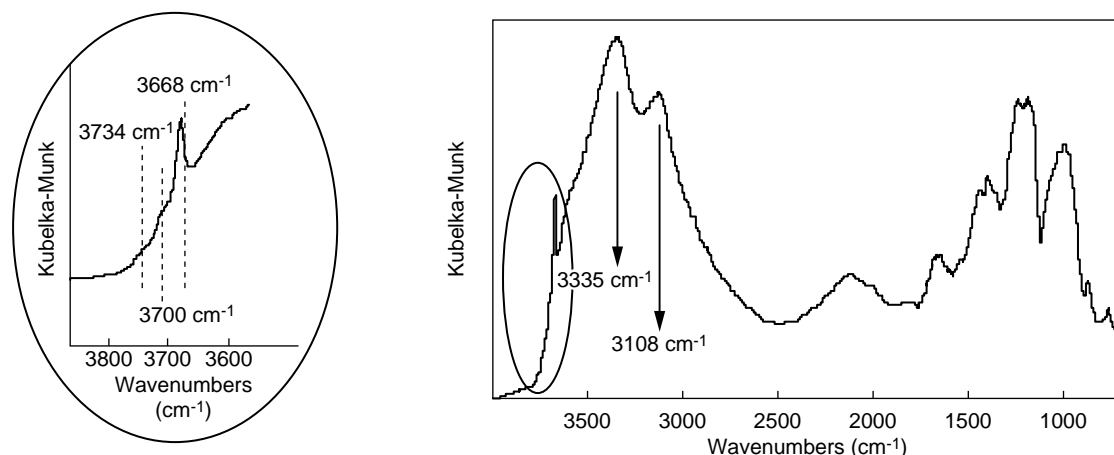
Figure 14

DRIFT spectrum of pure boehmite after one night under nitrogen at ambient temperature.

The following samples of boehmite with different Mo contents were prepared:

– Blank;
– nMo/nAl = 0.02;
– nMo/nAl = 0.123;
– nMo/nAl = 1.514.

Figure 15 shows the DRIFT spectra of all the samples after pretreatment overnight at 298 K under nitrogen blanket. The spectra are shown in Kubelka-Munk units and normalized to the band intensities at 2090 and 1970 cm^{-1} (attributed to the harmonics of the boehmite structure modes) in order to compare the band intensities of the different samples. The blank spectrum is consistent with that reported in the literature *(Fig. 15, a)* [22]. The bands at lower wave-number, at 1410 and 1360 cm^{-1}, are probably due to nitrate species present on the surface. Nitric acid was added during preparation to adjust the pH of the solutions. The same nitrates are not present in the spectra of the samples containing Mo *(Fig. 15, b, c and d)*. In this case the nitrates remain in solution and are removed by centrifugation.

In the OH stretching zone between 4000 and 2800 cm^{-1} in Figure 15, all the samples reveal two wide and intense bands at about 3335 and 3108 cm^{-1}, showing a slight shift towards lower wavenumbers and a change in the relative intensities depending on the Mo content. These bands were attributed respectively to the asymmetrical and symmetrical stretching vibrations of bulk hydroxyls. At higher frequencies, at 3570 cm^{-1}, the shoulder is present attributed to the stretching modes of the physisorbed water, and at about 1640 cm^{-1} the band corresponding to the δ(HOH) deformation mode.

In the region of OH group vibrations *(Fig. 16)*, for the blank *(Fig. 16, a)* intense absorption at 3668 cm^{-1} and two
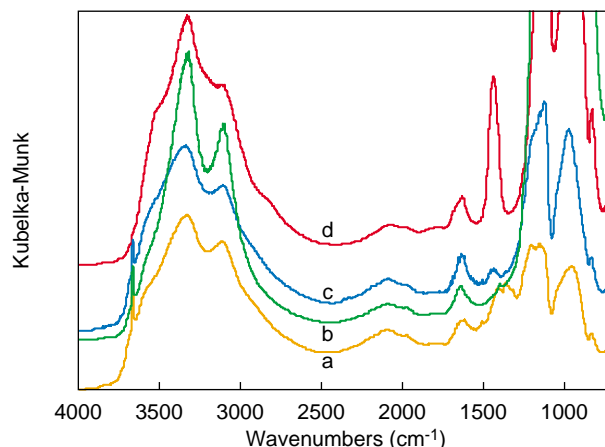

Figure 15

DRIFT spectra of all samples after one night at 298 K under nitrogen stream a) blank; b) 0.02; c) 0.123; d) 0.514.

main shoulders at 3700 and 3734 cm^{-1} can be observed. In agreement with the literature [12-14] these signals are attributed to the νOH of free hydroxyls of the OH groups present either on the basal faces of the boehmite (band at 3668 cm^{-1}), or on the lateral and positively charged faces (shoulders at 3700 and 3734 cm^{-1}). The relative intensity between the band of free hydroxyls at 3668 cm^{-1} and those corresponding to the structural OH at 3335 and 3108 cm^{-1} is typical of a crystalline boehmite with small particles. By increasing the Mo content, on the spectrum of the sample containing a Mo/Al molar ratio of 0.02 *(Fig. 16, b)*, the virtual disappearance of the signal at 3734 cm^{-1} is observed, with a decrease of the one at 3700 cm^{-1}. This finding tends to indicate that Mo is preferentially bonded to the OH of the
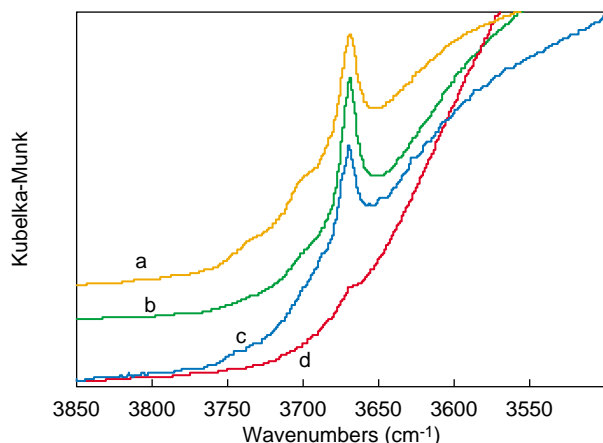
Figure 16

DRIFT spectra in the OH stretching region after one night at 298 K under nitrogen stream: a) blank; b) 0.02; c) 0.123; d) 0.514.

lateral faces. In the spectrum of 0.123 Mo *(Fig. 16, c)*, these two signals are no longer detectable. On the contrary, we are unable to determine whether a decrease occurs of the band due to the basal hydroxyls at 3668 cm^{-1}. This is because the spectra recorded in diffuse reflection can only be compared mutually from a strictly qualitative standpoint. The presence of physisorbed water, even if the spectra of the different solids have been recorded after the same pretreatment under nitrogen stream at ambient temperature, makes the comparison even more difficult. Finally, in the solid 0.514 Mo *(Fig. 16, d)* the band at 3668 cm^{-1} has also nearly disappeared and a very weak signal subsists. Hence there are no more free hydroxyl groups. These results confirm that the Mo introduced bonds preferentially with the lateral OH which are charged, and subsequently with the OH of the basal faces.

Recording of the spectra at elevated temperature (473 K) under nitrogen to eliminate traces of physisorbed water from the surface (the band at 1630 cm^{-1} has nearly disappeared) does not allow a better comparison between the OH bands because of the temperature effect on the bands, which broaden and slightly change the frequencies. If treatment at elevated temperature to remove the water is followed by lowering to ambient temperature, the boehmite surface traps a part of the water present in the nitrogen stream and the spectrum is identical to the one obtained after one night under nitrogen at 298 K.

Note also that the spectrum of the sample at higher Mo content recorded at ambient temperature *(Fig. 15, d)* displays a very intense band at 1421 cm^{-1}, already detectable in the spectrum of the solid at 0.123 Mo *(Fig. 15, c)*. This band is due to the NH$_4^+$ deformation modes of the species (NH$_4$)$_3$AlMo$_6$(OH)$_6$O$_{18}$ which is deposited on the support [20]. The stretching vibration bands corresponding to the

NH$_4^+$ group are masked by the wide structural OH bands between 3300-3000 cm^{-1}. Comparing this spectrum with that of (NH$_4$)$_3$AlMo$_6$(OH)$_6$O$_{18}$ shows most of the bands and, for example, the shoulder at about 2830 cm^{-1}. To confirm this assumption, the same samples were analyzed by Raman-FT spectroscopy. These results [21] are not presented here, but only the conclusions that can be drawn from there. The spectrum of the sample with 0.02 Mo displays a peak at 920 cm^{-1} which is characteristic, in agreement with reference [22], of the Mo = Ot stretching mode of the monomeric molybdate species, *i.e.* an Mo^{VI} in tetrahedral coordination. The significant shift of this Raman signal (from 898 for the free monomer to 920 cm^{-1} for the adsorbed material) attests to a strong interaction between the molybdate and the support surface. At higher Mo content, the spectrum of the sample 0.123, in addition to the peak of the monomer species, displays a new signal at 952 cm^{-1}. This may be due to a polymer species formed by the Mo-oxygen octahedra [23] and particularly to the symmetrical stretching mode of Mo = Ot of the typical Anderson structure, AlMo$_6$(OH)$_6$O$_{18}$$^{3-}$ [24]. The presence of this species is confirmed by the peak at 570 cm^{-1}, characteristic of the Al-O stretching of the same Anderson structure [25]. The Raman spectrum of the third sample with higher Mo content (0.514 Mo) only displays the peaks due to the Anderson structure (952 and 570 cm^{-1}) meaning that at this content, molybdenum is exclusively present in polymeric form widely dispersed on the surface. The results of the Raman analysis confirm the assumption made from the DRIFT spectra for this higher Mo content sample. However, the interaction of this species with surface OH has not yet been clarified.

As a partial conclusion, from these first measurements, it appears that with an increase in the Mo coverage, the coordination of the metal changes from mainly tetrahedral to octahedral as already observed for Mo/Al$_2$O$_3$ catalysts [17].

5.3 Conversion of Mo-Boehmite to Mo-Al$_2$O$_3$

Heating a boehmite above 750 K for a few hours causes dehydration leading to conversion to γ-alumina [3, 13]. The mechanism proposed considers that the decomposition of boehmite takes place through the removal of the water molecules resulting from condensation between the hydrogen atoms and the hydroxyl groups located on the neighboring layers, giving rise to the formation of γ-Al$_2$O$_3$. Based on NMR and thermogravimetry analyses, Fitzgerald *et al.* [26] concluded that the following processes occur at the different temperatures: desorption of physisadsorbed water between 323 and 423 K, dehydration due to the condensation of OH groups between 423 and 773 K, and above 773 K, a succession of dehydration and dehydroxylation. Our samples which contain Mo display the same type of behavior. ATD measurements were taken showing that regardless of the Mo content, a first endothermic peak occurs with a maximum

between 333 and 353 K, undoubtedly due to the loss of physisorbed water. A second signal at higher temperature is the consequence of the transition from AlOOH to γ-Al_2O_3. The temperature of this mechanism shifts from 710 to about 723 K depending on the Mo content, but the conversion is complete at 773 K in all cases.

Following these results, and using the detailed procedure in Table 1, each sample was heated in the DRIFTS cell from 298 K to 873 K at a constant rate of 10 K/min and under nitrogen, with plateaux. The surface spectra were recorded *in situ* at the end of each plateau ($T =$ cst).

TABLE 1

Sample heat treatment conditions

Initial temp. (K)	Final temp. (K)	Plateau (min)
298	353	10-45
353	473	10-45
473	573	45
573	723	45
723	873	45

Figures 17 and 18 show the spectra of the blank (0.0 Mo) at increasing temperatures. At 473 K *(Fig. 17, b)* the shoulder at 3570 cm^{-1}, attributed to the stretching modes of physisorbed water, and the lower wavenumber band at about 1640 cm^{-1}, corresponding to the deformation δ(HOH), have disappeared. This confirms the attribution of these bands and agrees fully with the ATG-ATD.

Looking at the change in the OH stretching bands with temperature *(Fig. 18)*, it may be observed that the conversion

of boehmite to γ alumina is terminated after 50 min at 873 K. This conversion is detectable from the structural OH stretching bands at 3335 and 3108 cm^{-1} which disappear as described above *(Fig. 18, f)*. Most of this conversion takes place at 723 K *(Fig. 18, d)*.

Contrary to the results reported in the literature [10, 27, 28], treatment at 723 K for 45 min does not appear to be sufficient to complete this conversion. It is in fact observed that the wide bands around 3400 and 3200 cm^{-1} are still present and that the OH stretching bands above 3650 cm^{-1}, typical of alumina, are not yet clearly defined *(Fig. 18, e)*. It is also observed that the effects of the broadening and wavenumber shift of the stretching bands with rising temperature are partly due to the conversion of boehmite to γ alumina, but also result from the temperature at which our *in situ* spectra were recorded. To overcome this effect due to heating, after 50 min at 873 K, the temperature was lowered to 298 K and a spectrum recorded *(Fig. 18, g)*. The bands corresponding to the stretchings of the alumina hydroxyls between 3600 and 3800 cm^{-1} are better defined and narrower, and their wavenumber positions change towards the typical values of an alumina. Unfortunately at this temperature, the sample adsorbs a portion of the water still present in traces in the nitrogen stream. This is confirmed by the formation of a wide medium-intensity band below 3600 cm^{-1}. This is why, even if the spectra are modified due to the temperature, the spectra recorded at high temperature are considered.

The temperature behavior of the samples containing Mo is similar to that already observed for the blank. For these solids also, it is necessary to vary the temperature to 873 K for the conversion to γ alumina to be complete *(Figs. 19, 20*
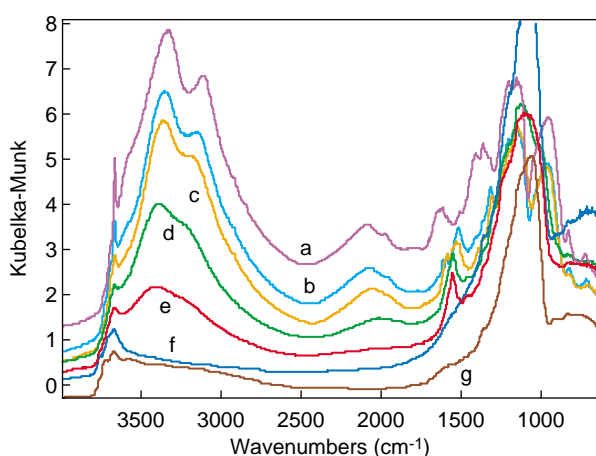

Figure 17

DRIFT spectra of blank (0.0 Mo) with temperature a) after one night at 298 K; b) 45 min at 473 K; c) 45 min at 573 K; d) 10 min at 723 K; e) 45 min at 723 K; f) 50 min at 873 K and g) lowering to 298 K (spectra in common scale).
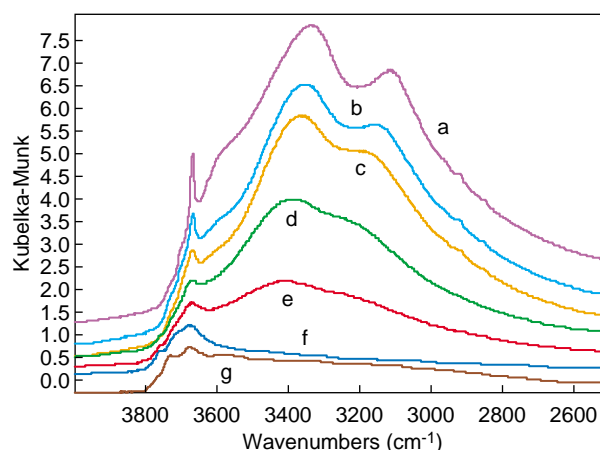

Figure 18

DRIFT spectra in the stretching OH region of blank (0.0 Mo) with temperature. a) after one night at 298 K; b) 45 min at 473 K; c) 45 min at 573 K; d) 10 min at 723 K; e) 45 min at 723 K; f) 50 min at 873 K and g) lowering to 298 K (spectra in common scale).
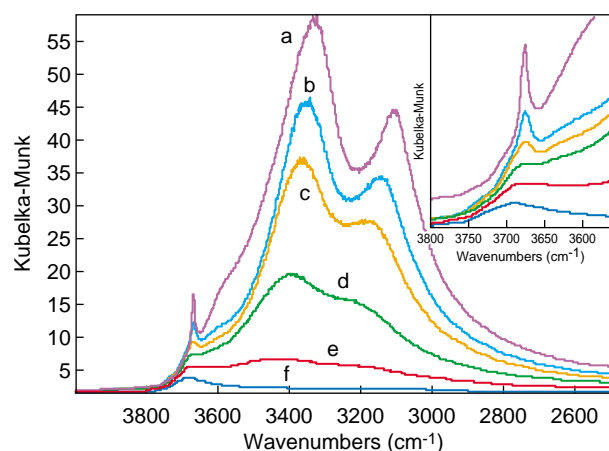
Figure 19

DRIFT spectra in the OH stretching region for the 0.02 Mo sample with temperature. a) after one night at 298 K; b) 60 min at 473 K; c) 10 min at 573 K; d) 10 min at 723 K; e) 45 min at 723 K; f) 50 min at 873 K.
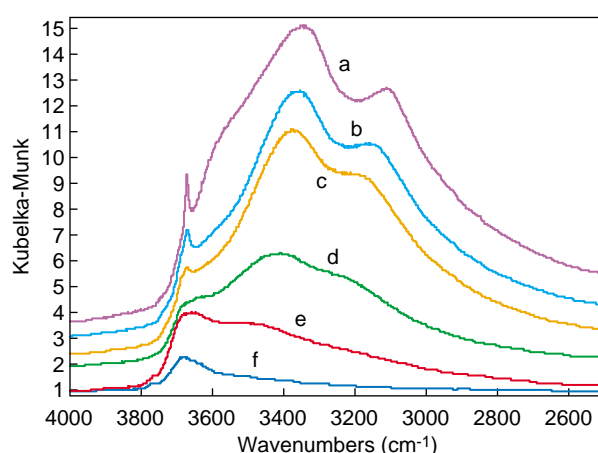

Figure 20

DRIFT spectra in the OH stretching region for the 0.123 Mo sample with temperature. a) after one night at 298 K; b) 60 min at 473 K; c) 10 min at 573 K; d) 10 min at 723 K; e) 50 min at 723 K; f) 45 min at 873 K.

and 21). The different metal contents seem to have little effect on this conversion, at least where the final temperature is concerned, even though with the highest Mo content sample (0.514 Mo) after 45 min at 723 K, the process already appears to be complete *(Fig. 21, e)*. These results show good agreement with those of ATD-ATG. Note that in the case of the sample at 0.514 Mo *(Fig. 21)* the band at 1434 cm^{-1} of the δNH_4^+, of the species $(NH_4)_3AlMo_6(OH)_6O_{18}$ disappears at 573 K (this is consistent with the fact that this species decomposes above 473-573 K to $Al_2(MoO_4)_3 + MoO_3$) [22].

On the γ alumina spectra obtained in the DRIFTS cell after temperature conditioning (45 min at 873 K) under nitrogen stream, substantial differences are observed between the samples which contain different Mo contents *(Fig. 22)*. In all cases, the bands are fairly broad, which is partly due to the temperature effect.

The typical infrared spectrum of a γ alumina displays at least four bands in the hydroxyl group stretching zone. A small shoulder at 3790 cm^{-1} (terminal OH on an Al in tetrahedral coordination with a non-vacant environment), a
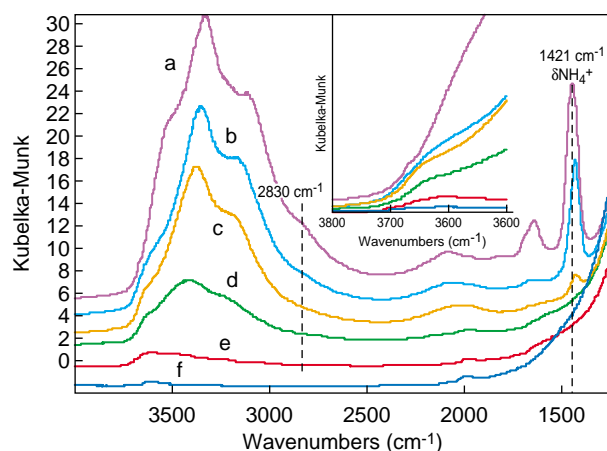

Figure 21

DRIFT spectra of the 0.514 Mo sample with temperature. a) after one night at 298 K; b) 60 min at 473 K; c) 45 min at 573 K; d) 10 min at 723 K; e) 45 min at 723 K; f) 45 min at 873 K.
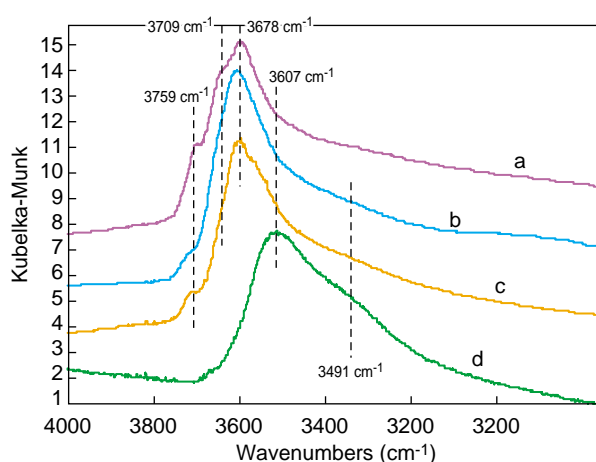

Figure 22

DRIFT spectra in the OH stretching region of samples after treatment at 873 K for 45 min under nitrogen stream. a) blank; b) 0.02; c) 0.123; d) 0.514.

band at 3770 cm^{-1} (terminal OH on an Al ion in tetrahedral coordination near a cationic vacancy), 3730 cm^{-1} (terminal OH on an Al ion in octahedral coordination), 3680 cm^{-1} (bridged OH) and possibly a weaker and broader band at 3590 cm^{-1} (triple bridged OH) [29]. The spectrum of our blank shows three main bands in the region of the OH stretchings at 3759 cm^{-1} (weak), 3709 cm^{-1} (shoulder) and 3678 cm^{-1} (strong) *(Fig. 22, a)*. These bands can be attributed respectively to the stretching modes of the terminal OH on the Al ions with tetrahedral coordination (3759 and 3709 cm^{-1}) and to the bridged hydroxyls (3678 cm^{-1}). The shift towards lower wavenumbers observed in our case can be attributed to the temperature at which the spectrum was recorded (873 K).

The DRIFT spectra of aluminas at different Mo contents reveal the progressive disappearance or frequency shift of certain OH vibration bands as a consequence of the initial interaction of the metal with the hydroxyl groups of the original boehmite surface. In the spectrum of the sample at lowest Mo content (0.02 Mo), the shoulders at 3759 and 3709 cm^{-1} have nearly completely disappeared and a weak band is detectable at 3769 cm^{-1} *(Fig. 22, b)*. At higher Mo loading all the hydroxyl groups have practically disappeared, and are supplanted by a wide band with a maximum at about 3607 cm^{-1} characteristic of some hydroxyls either structural or hydrogen bonded *(Fig. 22, d)* [17].

If the spectra of the same aluminas are recorded in transmission (FT-IR) at ambient temperature, the same pattern of band variation with Mo content is also observed *(Fig. 23)*. The OH bands are better defined, owing to the lower acquisition temperature. In the case of alumina (0.0 Mo), weak signals at 3790 and 3590 cm^{-1} can also be distinguished, the latter attributed to a triple bridged OH *(Fig. 23, a)*. The differences observed between these samples with rising Mo content in the hydroxyl group vibration bands are comparable to those already observed for diffuse reflection infrared spectra. Mo interacts with the alumina surface hydroxyls, progressively causing a decrease in the intensity of the bands corresponding to the OH stretching as a function of metal content. It is clear that the highest frequency OH band is eliminated first *(Fig. 23, b)*. This band is attributed to the most basic hydroxyl group [18, 30] which, according to previous studies on Mo/Al$_2$O$_3$ type catalysts [15-21], appears to be the preferred interaction site for the molybdate anion. The bands at 3730 and 3680 cm^{-1} appear to decrease at the same rate as already observed by [21].

The disappearance of the band at 3770 cm^{-1} (from the 0.02 Mo sample), simultaneous with a shift in the band from 3780 to 3785 cm^{-1}, is also noteworthy. Although the same mechanisms are also present in the case of Mo/Al$_2$O$_3$ catalytic materials [17], they have heretofore not been taken into consideration. In our case, at lower Mo content, an explanation can be suggested if we consider the topotactic
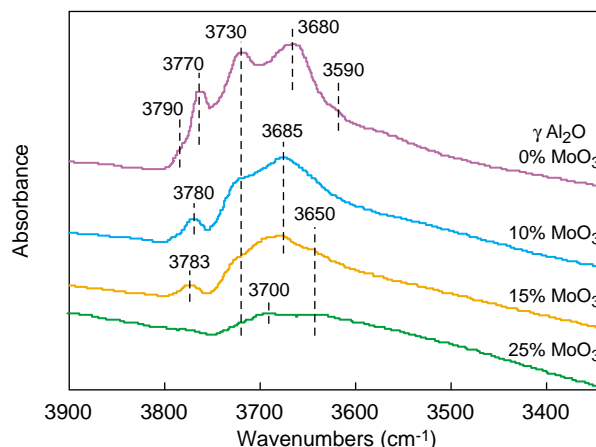

Figure 23

FT-IR spectra in the region of the OH stretching of the different aluminas with growing Mo content observed on the corresponding boehmites treated and converted during the tests.

nature of the AlOOH → γ-Al$_2$O$_3$ conversion. If the location of the molybdate on the γ-Al$_2$O$_3$ is inherited from that of the boehmite, the molybdate should mostly be located on plane (001) of the γ-Al$_2$O$_3$ (and which is derived from face (100) of boehmite) and on face (1-10) occurring from plane (001) of the boehmite. The band at 3775 cm^{-1} could correspond to the OH groups located on face (001) of the γ alumina according to the *ab initio* calculations performed by Digne *et al.* [31]. This attribution would explain the loss of the OH vibration band at about 3775 cm^{-1} which is observed when a small amount of Mo is added. These results appear to agree closely with those already reported by Morterra [32] and Srinivasan [33] who emphasized the strong reactivity of these hydroxyls. On the contrary, the nature of the band at 3680/3685cm^{-1} is still debatable.

In conclusion, it emerges from this study that:

– at low Mo content, the Mo first interacts with the charged lateral OH;
– the presence of Mo at the boehmite surface slightly modifies the boehmite → alumina conversion temperatures;
– DRIFT and FT-IR spectra of alumina at different Mo contents display the same pattern of bands observed for conventional Mo/Al$_2$O$_3$ catalysts, in the region of the OH group stretchings.

5.4 Effect of Ionic Strength

The final point of this study on boehmites raises the question as to the specific type of interaction between molybdate and boehmite (electrostatic, iono-covalent, hydrogen bond). The decreased intensity of the OH stretching band could indicate that this interaction is stronger than a simple electrostatic mechanism (ionic strength). In order to assess the potential

influence of ionic strength and its effect on the infrared spectra, the solids listed in Table 2 were investigated.

IR 2	Boehmite sol - ionic strength I = 0 M (molar)
IR 3 0.1 M NaNO$_3$	Boehmite sol - ionic strength I = 0.1 M (molar)
IR 0.01 M NH$_4$NO$_3$	Boehmite sol - ionic strength I = 0.01 M (molar)
IR 0.1 M NH$_4$NO$_3$	Boehmite sol - ionic strength I = 0.1 M (molar)

For each solid, after pretreatment overnight under nitrogen stream at 298 K, the temperature was raised to 473 K at the rate of 10 K/min with a plateau of 40 min at 353 K.

A comparison with the different spectra recorded at 353 K *(Fig. 24)* shows the absence of any appreciable variations in the zone of the OH stretching modes. None of the OH bands, either structural (3121 and 3440 cm^{-1}), nor of the basal (3668, and at 3672 cm^{-1}) and lateral (3699 cm^{-1}) faces, appear to undergo any change. It would appear that the lateral OH band at 3734 cm^{-1} disappears in the case of the highest ionic strength *(Fig. 24, c)*, but since this signal is very weak and broad, this finding may be questionable. This experiment shows that the decreased intensity of the OH bands in boehmites containing Mo does not derive from a simple electrostatic interaction. A more specific interaction must exist.
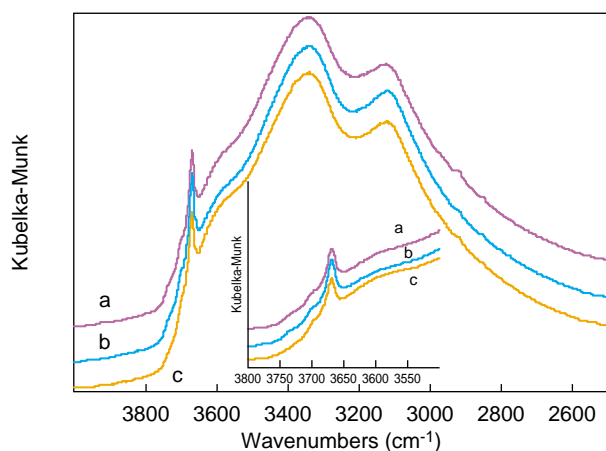

Figure 24

DRIFT spectra in the OH stretching region after 10 min at 353 K under nitrogen. a) blank; b) IR 0.01 M NH$_4$NO$_3$; c) IR 0.1 M NH$_4$NO$_3$.

6 APPLICATION OF DRIFTS SPECTROSCOPY AT ELEVATED TEMPERATURE UNDER REACTIVE ATMOSPHERE

The study went on to investigate materials under reactive atmosphere. To address this topic, it was decided to study the

adsorption and reduction of nitrogen oxide molecules on different materials and in different reaction conditions (temperature, flowrate and type of atmosphere). Nitrogen oxides were selected for the study because these gases, emitted by automobile vehicles and industry, are toxic and harmful to the environment. Nitrogen oxides (NO$_x$) are increasingly present in urban atmospheres and are hence monitored. For automobiles, ever stricter standards are being promulgated, and since 1993, gasoline vehicles have been equipped with "three-way" catalytic converters, simultaneously removing NO$_x$, unburnt hydrocarbons and carbon monoxide (CO).

Diesel engine vehicles, which are in principle less polluting, are now equipped with catalytic oxidation converters to remove CO and unburnt hydrocarbons, but not NO$_x$. Forthcoming European standards will nonetheless impose the development of a process to eliminate released NO$_x$. The solution adopted for gasoline vehicles (three-way catalysis) is ineffective for Diesel engines (as well as the new "lean burn" engines) because the proportion of oxygen in the Diesel exhaust gases is much higher (5 to 15 against 0.2 to 2%). Since the ambient environment is oxidizing, the reduction of NO$_x$ becomes difficult.

In the early 1990s, the first catalyst was discovered for reducing NO$_x$ ("DeNO$_x$ catalyst") by a hydrocarbon (assumed to be unburnt leaving the engine or directly injected into the catalytic converter) in oxidizing medium. Since then, many catalyst systems have been proposed for this reaction. They can be classed in three main categories:
– zeolites exchanged by metals;
– metallic oxides;
– noble metals, particularly supported platinum.

To assess the activity of materials, which are potential NO$_x$ reducing catalysts, with hydrocarbons in oxidizing medium, an analytical system was developed designed to combine tracking catalyst reactivity with analysis of the gas phase by infrared and/or mass spectrometry, and direct observation of the species present on the catalyst surface in reaction conditions by *in situ* infrared spectroscpopy. Initially, it was intended to identify the N$_x$O$_y$ species adsorbed on the surface of the materials as a function of temperature, track their thermodesorption, and subsequently monitor the adsorption of NO$_x$ at different temperatures during regeneration of the catalyst by hydrocarbon pulses.

Since many of theses materials transmit very little or no IR radiation, in the nitrogen oxides region, it is necessary to resort to diffuse reflection infrared spectroscopy using the DRIFT cell *in situ* at high temperature and pressure. An apparatus was designed and assembled to prepare gas mixtures in desired proportions, and send them to the DRIFT cell. The following mixtures were used:
– 10% O$_2$ in argon for catalyst pretreatment or to dilute the NO;

– 600 to 1700 ppm NO in a 10% O_2/Ar mixture (lean phase);
– 1600 to 4800 ppm propylene (C_3H_6) diluted in argon (rich phase).

The total flowrates ranged between 25-50 cc/min. The materials, first pretreated (phase zero), were subjected to two different atmospheres, and two distinct configurations (phases 1 and 2) were provided for:

phase 0: pretreatment at 873 K under O_2/Ar stream for 2 h;

phase 1: NO_x adsorption at different temperatures followed by thermal desorption under O_2/Ar stream;

phase 2: NO_x adsorption at different temperatures with regeneration by hydrocarbon pulses.

This apparatus is well adapted to the study of NO_2 trappers which work sequentially thanks to an adapted engine control.

6.1 Description of the Gas Feed Assembly

Figure 25 shows the fluid portion of the gas mixer. It comprises:
– gas inlets;
– two series of valves, manual and solenoid;
– 7 μm filters;
– mass flowmeters;
– two valves, one four-way and one six-way, to allow the gas mixtures into the DRIFTS cell, making it possible to impose openings and closures at given time intervals and to create cycles.

This assembly makes it possible to monitor the type, concentration and flowrate of the gas streams passing through the cell containing the sample. The figure below shows one of the four possible combinations of positioning the two four- and six-way valves.

For the first nitration experiments at elevated temperature, a cell designed to analyze the gas mixtures by infrared spectroscopy was mounted at the outlet of the DRIFT cell *(Fig. 25)*. The gas cell was placed in an ancillary compartment of the same infrared spectrometer. Since the cell volume was fairly large (about 50 cc), it was nonetheless difficult to perform quantitative assessments, so that the exit gases were only subjected to qualitative analysis.

6.2 DeNO$_x$ Catalysts (Nitration at Constant Temperature)

The first tests were conducted on two reference materials: a sample of composition Ba/Al$_2$O$_3$ (160 m^2/g, 18% w/w Ba, loading 0.4), and a sample containing platinum Pt/Al$_2$O$_3$. The first experiments, on each product, consisted of nitration at different temperatures ($T_{nitration}$) followed by desorption at rising temperature (TPD).

The sample is first pretreated for 2 h at 873 K under a stream of 25 cc/min composed of 10% O_2 in Ar. After the 2 h interval, the temperature is lowered to $T_{nitration}$. Nitration takes place by adding 600 ppm NO into the pretreatment gas stream. During nitration, a DRIFT spectrum of the surface, with a single beam, is recorded every 5 min. After 1 h of nitration, the NO intake is cut off and replaced by a stream of O_2 + Ar. After about 30 min at $T_{nitration}$, the sample is
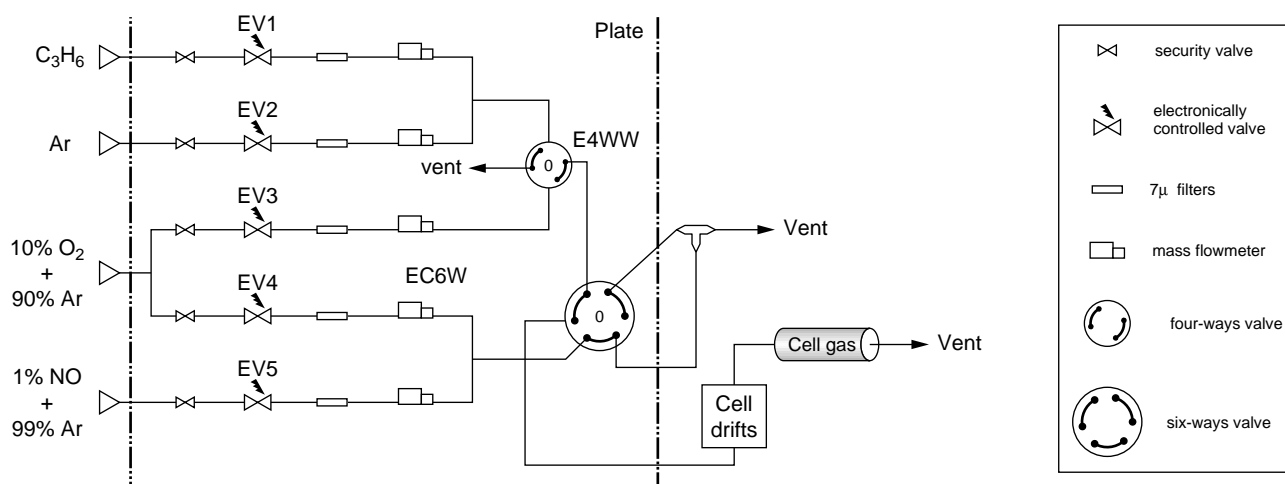

Figure 25

Complete gas mixer with gas cell.

progressively heated to 873 K (at 5 K/min) to analyze the stability of the species formed. During desorption, a surface spectrum is recorded every 5 min.

The following nitration temperatures were considered: 423, 473, 573 and 673 K. From the operating standpoint, note that the $NO + O_2 + Ar$ mixture must be stabilized before being sent to the cell. This is why, during pretreatment of the sample under $O_2 + Ar$, the mixture containing NO circulates and is sent to the vent for about 1 h. A check is performed to ensure that the intensities of the infrared bands (proportional to the respective concentrations) of NO and NO_2 remain constant. By adjusting the position of the four- and six-wave valves, the gas phases containing NO and containing no NO can be sent to the cell alternately *(cf. Fig. 27).*

6.2.1 Ba/Al$_2$O$_3$, Nitration at Different Temperatures

As an example, the diffuse reflection spectra during 1 h of nitration at 573 K are shown in Figure 26. These spectra, from reprocessed single beam data, were obtained using as a background the single beam spectrum of the activated catalyst surface recorded just before nitration (at $T_{nitration}$). The spectra thus directly show the bands of the species present at the material surface. The presence of structural bands of the sample below 1100 cm^{-1} limits the useful spectral region to 4000 to 1100 cm^{-1}. The spectra are always presented in common scale. Various procedures are available for reprocessing the spectra, and the ideal one is still subject to debate. The DRIFT spectra shown here were all obtained using the activated surface of the catalyst at a given temperature as the *background*.

From the first spectrum at the start of nitration ($t = 0$ min) which displays no signal, Figure 26 shows the formation of a series of bands of variable intensity over time. After 5 min, a

band at 1230 cm^{-1} due to the presence of nitrite species on the surface appears. The nearly exclusive formation of nitrites is initially observed. After 30 min the spectrum displays a very weak signal at 1475 cm^{-1} due to the incipient formation of nitrate species.

During nitration the nitrate bands (a shoulder at 1308 cm^{-1} and the band at 1475 cm^{-1}) increase in intensity, but still remain weak. After 40 min, the nitrite band remains constant.

The pattern of the spectra is different at 673 K *(Fig. 27).* In this case, we initially observe the formation of nitrites (band at 1229 cm^{-1}), followed by the appearance of nitrates (1485 and 1296 cm^{-1}). Unlike the previous experiments, the bands corresponding to nitrates become increasingly intense and the gradual disappearance of the nitrite bands is simultaneously observed. After 1 h of nitration only nitrate species are found on the catalyst surface. The quantity of nitrite species goes through a maximum after about 20 min of nitration. In general, the quality of the spectra is observed to be increasingly weak with rising nitration temperature because the diffusion of the IR beam on the sample decreases with increasing temperature, so that the signal-to-noise ratio decreases.

Let us consider the changes in the species on the catalyst surface during de-nitrations at rising temperature (TPD). After 1 h of nitration, the NO stream is cut off and the sample heated from $T_{nitration}$ to 873 K under $O_2 + Ar$. This desorption phase is monitored by analyzing changes in the spectra of the species present either on the catalyst surface by DRIFTS, or in the gas phase. The spectra of the surface and of the gases leaving the DRIFTS cell are recorded every 5 min. It is complicated to analyze the change in the bands of the species present on the catalyst surface because of the diffusion of the IR beam, which evolves as a function of temperature and
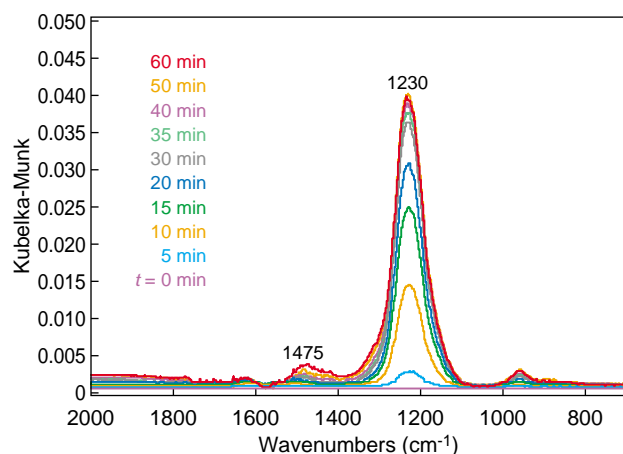
Figure 26

Ba/Al$_2$O$_3$, DRIFT spectra of nitration at 573 K, variation in bands during 1 h (activated surface background) (spectra in common scale).

Figure 27

Ba/Al$_2$O$_3$, DRIFT spectra of nitration at 673 K, variation in bands during 1 h (activated surface background) (spectra in common scale).

Figure 28

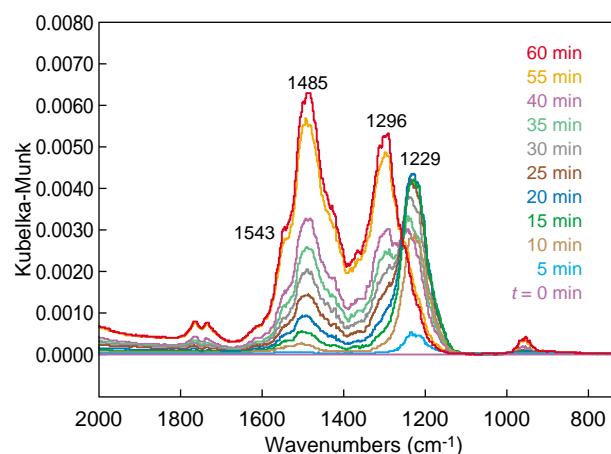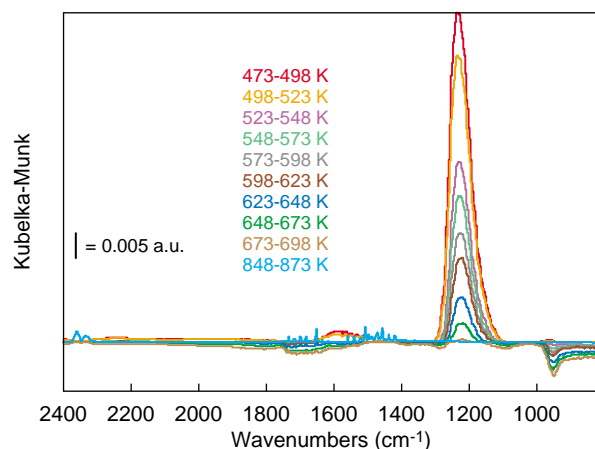Ba/Al$_2$O$_3$, DRIFT spectra of de-nitration (under O$_2$ + Ar), variation in bands from 473 to 873 K (activated surface background at the same temperatures) (spectra in common scale).
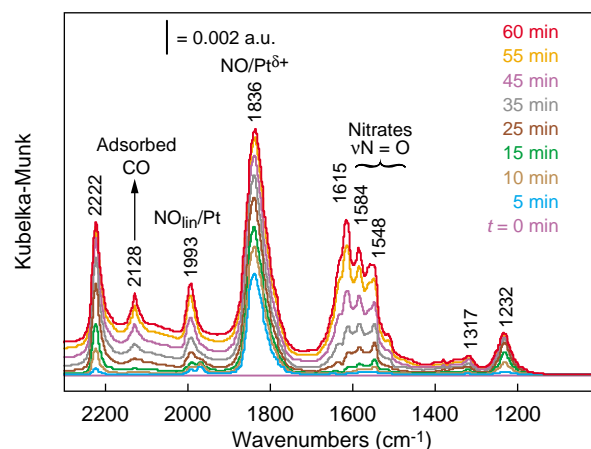

Figure 29

Pt/Al$_2$O$_3$ DRIFT spectra, variation in species at the surface during 1 h of nitration at 423 K (background first spectrum, activated surface) (spectra in common scale).

which alters the ratios of the band intensities. Given the difficulty of introducing correction factors, this analysis is not highly relevant in most cases. However, as an example, Figure 28 shows the desorption spectra after nitration at 473 K on Ba/Al$_2$O$_3$. As expected, the only change concerns the nitrite band around 1230 cm^{-1} which disappears. The surface is restored from 700 K.

In this type of desorption (de-nitration) analysis, the surface spectra (recorded with single beam and at variable temperature) were processed with the (single beam) spectra of the initial surface recorded at the same temperatures.

6.2.2 Pt/Al$_2$O$_3$, Nitration at Different Temperatures

Figure 29 shows the variation in species of the catalyst surface (Pt/Al$_2$O$_3$) during 1 h of nitration at 423 K. From the first few minutes, a series of bands appears, increasing in intensity during the experiment up to 55 min of nitration. The bands at 1548 and 1584 cm^{-1} can be attributed to νN = O vibrations of the nitrate species [34] and the intense band at 1836 cm^{-1} to linear NO on the oxidized platinum [35-37]. It is more difficult to attribute the bands of 1615 and 1993 cm^{-1}. The band at 1993 cm^{-1} could result from the adsorption of NO linearly on Pt(II+) [33]. At this temperature, in our system, a small quantity of CO is present. The bands at 2128 and 2222 cm^{-1}, respectively attributable to CO$_{lin}$/Pt and AlNCO [33, 38], appear to confirm this.

As to the experiments at high temperature: during nitration at 473 K, the changes in spectra of the species at the surface are quite similar to those at 423 K. The bands are the same, the same frequencies, and only the nitrate bands are relatively more intense.

The formation of a single very intense and complex band is observed at 573 K with a peak at 1582 cm^{-1}, a shoulder at 1563 cm^{-1} and less clearly defined shoulders at 1610 and 1629 cm^{-1} *(Fig. 30)*. This band increases progressively and steadily over time and after 1 h, it is impossible to state whether the maximum intensity has been reached. Weak signals are also detectable around 1850 and 2221 cm^{-1}. The same behavior is observed in the case of nitration at 673 K, the peak of the band occurring at 1577 cm^{-1} with a main shoulder at 1610 cm^{-1}. Contrary to what was hitherto observed, at this temperature the nitrate band grows more rapidly in the first minutes of nitration, and after half an hour, appears to have reached the maximum intensity. The
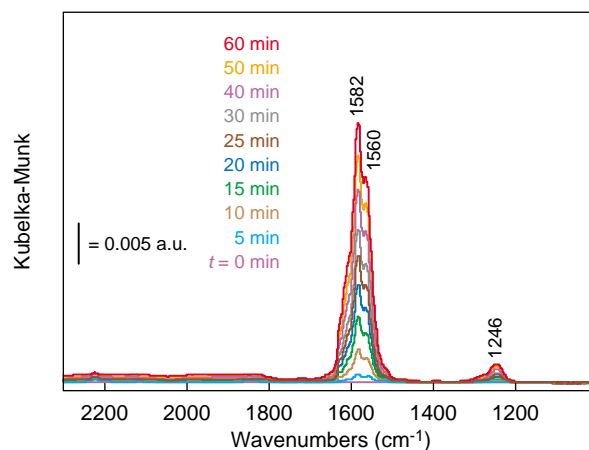

Figure 30

Pt/Al$_2$O$_3$, DRIFT spectra, variation species at the surface during 1 h of nitration at 573 K (background first spectrum, activated surface) (spectra in common scale).

intensity of the bands at 1850 and 2221 cm^{-1} is always very weak. No further information was obtained from the analysis of the gases leaving the DRIFTS cell.

7 ANALYSIS OF CATALYSTS UNDER REACTIVE ATMOSPHERE: NITRATION AND REGENERATION BY HYDROCARBON PULSE

We then investigated the regeneration of the surface by hydrocarbon pulses.

Experimental Conditions

Operating procedure:

Pretreatment conditions
– temperature rise from 298 to 873 K (10 K/min) with flushing by an oxygen/argon mixture (10% O_2 in Ar, 50 cc/min);
– plateau of 2 h at 873 K under O_2/Ar;
– lowering to T_i (O_2/Ar) recording of reference spectrum (single beam).

Nitration and regeneration by hydrocarbon pulses (propylene conditions):
– at T_i = cst (423, 498, 573, 648 and 723 K) switching of richness between lean phase (1700 ppm NO in O_2/Ar, total flowrate 50 cc/min) and rich phase (2000 ppm C_3H_6 in Ar, total flowrate 50 cc/min) every 3 min;
– ten cycles at each temperature (1 h of analysis);
– recording of a spectrum every 3 min, just before each switchover.

The series of cycles was used to have a uniform response of the system. The different plateaux succeed each other on the same experiment and the temperature between T_i and T_{i+75} is increased at the rate of 10 K/min (under O_2/Ar). The same procedure is repeated over two separated experiments: first only the species on the surface are analyzed (diffuse reflection spectrum) and during the second experiment only the gases leaving the DRIFTS cell ("on-line" gas cell). The successive experiments on the same sample are considered to yield repeatable and consistent results.
– DRIFTS analysis: processing of the spectra using as a background the single beam spectrum of the catalyst surface at T_i under O_2/Ar just before starting the cycles.
– Gas analysis: recording of transmission spectra using as background the spectrum of the cell under O_2/Ar (recording of reference spectrum daily before starting the experiment).

Case of Ba/Al$_2$O$_3$

Figure 31 shows the DRIFT spectra of the species on the surface of Ba/Al$_2$O$_3$ during the ten richness switching cycles

at 573 K. These profiles were obtained by reprocessing the single beam spectra with the activated catalyst spectra, recorded at 573 K under O_2/Ar stream. At each cycle, one spectrum (respectively of the surface (DRIFTS) or of the gas phase leaving the cell (FT-IR)) was recorded. To guarantee equilibrium conditions, the spectra were obtained after 3 min of flushing (lean phase and rich phase respectively), before the next switchover. The figure only shows the most significant cycles. As in the case of simple nitration, some change in the bands is observed during 1 h of treatment. During the first cycle under lean phase (NO/O_2/Ar mixture blanket) two bands appear, one very low intensity at 1609 cm^{-1} and a second more intense band at 1225 cm^{-1}. The second can be attributed to a nitrite species, as previously observed in the case of simple nitration, while the higher wavenumber band could be an indication of the formation of nitrates or carbonate or hydrogeno-carbonate species [M --- C(CO)OH], because of the presence of CO_2 (corresponding bands in the gas phase, *Fig. 32*). During the rich phase (C_3H_6/Ar mixture) these two bands increase in intensity (especially the one at 1609 cm^{-1}) indicating that at this stage of the experiment, the nitrites accumulate and are not yet converted. In the next two cycles, the nitrite band continues to increase in intensity. From the fourth cycle (24 min of test) the nitrite band increases in lean phase and decreases in rich phase. The decrease in this band under propylene stream reveals some activity of the catalyst at this temperature. Either the nitrites become nitrates (as observed during the nitration test) or they are converted to organo-nitrate species. In fact, two weak bands appear at 2166 and at 2234 cm^{-1}, which can be attributed respectively to cyanide and isocyanate species associated with Ba [39]. Their intensities remain weak (even at the end of the tenth cycle). Even if the band at 1225 cm^{-1} decreases in intensity, it does not disappear, indicating that a large portion of the nitrites do not react. The band at 1609 cm^{-1}, however, seems to belong to a species, either nitrate or hydrogeno-carbonate or other, much more stable and which accumulates on the surface. In Figure 32, the absorbance spectra of the gases leaving the cell and corresponding to the same experiment are plotted. At each cycle, in the lean phase, in addition to the feed gases (NO, NO_2, N_2O), the presence of CO_2 is observed, the band intensity of which increases during the ten cycles. Even with a C_3H_6/Ar stream, the quantity of CO_2 increases, which is clearly to be expected. CO_2 affects the combustion of propylene, which appears to increase with time, reaching equilibrium after half an hour of test: the CO_2 concentration in the rich phase remains virtually constant. However, since a quantification of the species is not possible, our discussion is restricted to qualitative and relative quantitative considerations.

After 1 h of richness switchover at 573 K, the temperature is raised to the next plateau (648 K) at the rate of 10 K/min, under O_2/Ar stream (50 cc/min). Before starting the same
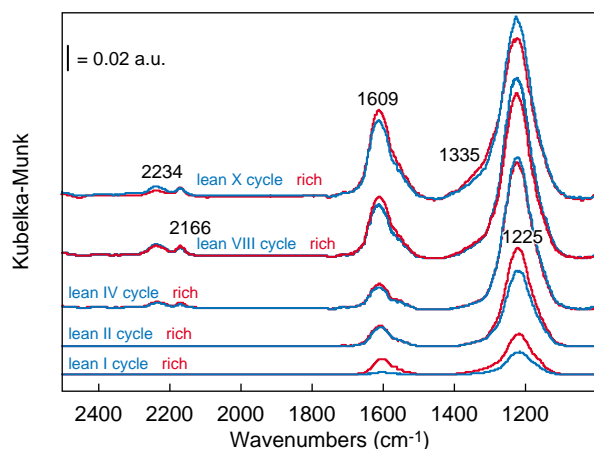
Figure 31

Ba/Al$_2$O$_3$ DRIFT spectra of the surface during 1 h of richness switchovers (lean phase (blue); rich phase (red)) at 573 K (spectra in common scale).

Figure 32
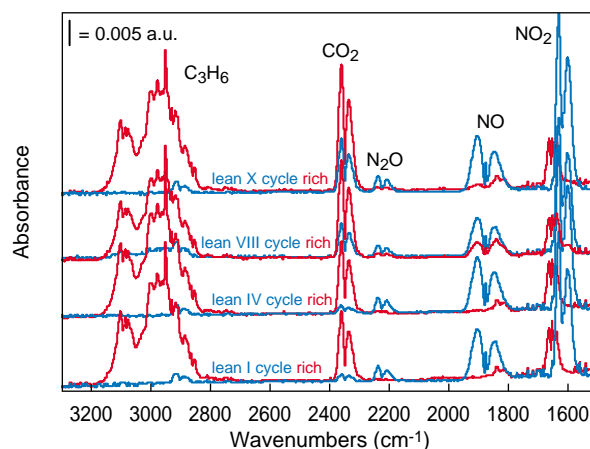
Ba/Al$_2$O$_3$ FT-IR spectra of the gas phase leaving the cell during 1 h of richness switchover (lean phase (blue); rich phase (red)) at 573 K (spectra in common scale).

experiment at this temperature, the surface spectrum is recorded, to serve as a reference to reprocess the successive spectra. Observation of the surface state at 648 K *(Fig. 33, a)* shows that some species remain adsorbed on the catalyst, which have accordingly resisted the heat treatment under O$_2$. Two bands can be distinguished, a very intense band at 1227 cm^{-1} and a second less intense band at 1609 cm^{-1}. Nitrites and nitrates (or hydrogeno-carbonates) are still present on the surface, but the cyanates and isocyanates have been eliminated (bands at 2166 and 2134 cm^{-1}).

Figure 34 shows the species corresponding to the cycles at 648 K. During the first cycles, the quantity of nitrite increases during the lean phase (cf. the band at 1228 cm^{-1} grows in intensity) and then decreases in the rich phase, either due to the hydrocarbon or because they are converted to nitrates. From the fourth cycle, two bands appear at 1301 and about 1431 cm^{-1} which seem to correspond to the bands of nitrates formed during the simple nitration experiments *(Fig. 26)*. By simultaneously analyzing these two experiments, we find the same pattern. The nitrites formed initially are then converted
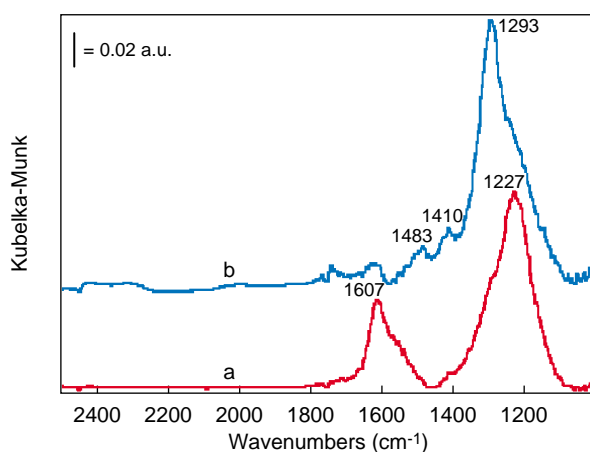

Figure 33

Ba/Al$_2$O$_3$ DRIFT spectra of the surface under O$_2$/Ar before the test, a) at 648 K; b) at 723 K (spectra subtracted from the surface of the start of the experiment at 573 K; common scale).
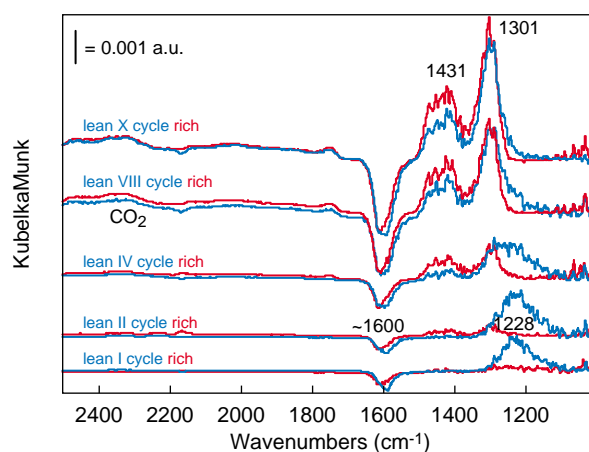

Figure 34

Ba/Al$_2$O$_3$ DRIFT spectra of the surface during 1 h of richness switchovers (lean phase (blue); rich phase (red)) at 648 K (spectra in common scale).

to nitrates (more stable). From the sixth cycle on there is virtually no formation of the nitrite band, but the bands at 1301 cm^{-1} and 1430 cm^{-1} increase steadily in intensity at each cycle. Hence at this stage we probably observe the direct formation of nitrates. At the same time, a very weak signal, due to gaseous CO_2, appears around 2350 cm^{-1}. Note also the appearance of a negative band at about 1600 cm^{-1} which increases in intensity after 1 h. This negative band is a consequence of the removal of the species (carbonate, nitrate or other) which remained attached to the surface after the test at 573 K and which is no longer stable at 648 K. Also observed is the absence, in this experiment, of the two bands around 2166 and 2234 cm^{-1}.

The gas phase spectra provide us with no new data and the band pattern is perfectly comparable to that of Figure 32. The quantity of CO_2 increases during the operation, in lean or rich phase. It can be concluded that at 648 K we first observe the formation of nitrites which are converted to nitrates, and at the same time, the disappearance of certain species which remained on the surface from the previous test. Moreover, no formation of organo-nitrate species was observed.

Analysis of the catalyst spectrum at 723 K before starting the next steps (spectrum recorded under O_2/Ar after the test at 648 K) *(Fig. 33, b)*, shows that the composition of the bands remaining on the surface has changed. The band at 1607 cm^{-1} has nearly disappeared and instead of the band at 1227 cm^{-1} we find a very intense band at 1293 cm^{-1}, as well as low intensity bands at 1410 and 1483 cm^{-1}. These concern species that are either nitrates, or carbonates which are stable enough to remain on the surface at this temperature.

The spectra obtained from the test at 723 K are shown in Figure 35. The band pattern is relatively similar to the one described for the test at 648 K, but some differences must be emphasized. As at the lower temperatures, a nitrite band at 1225 cm^{-1} increases during the lean phase of the first cycles and disappears under the rich mixture at the same time as the formation and increase of the band at 1300 cm^{-1}. After about 40 min of switchover, the nitrites at 1225 cm^{-1} no longer appear. The band at 1300 cm^{-1} increases in intensity under lean mixture and decreases under a rich mixture, and new bands emerge at 1395 and 1480 cm^{-1}. At higher wave-numbers, the band of the species at 1600 cm^{-1} appears to form initially under a rich mixture and then decreases in a lean phase and during the experiment. In the final cycle it is no longer formed. More interesting is the behavior of the two bands at 2164 and 2224 cm^{-1}. These bands, attributed to barium cyanates and isocyanates, had already been observed during the test at 573 K, where they displayed a weak but constant intensity. At 723 K, by contrast, these bands have a medium and decreasing intensity over time, but more importantly, they completely disappear during each lean phase and are re-formed under rich phase. This could mean that at this temperature the NO_x are partially reduced *via* cyanates and isocyanates. The confirmation of this possibility
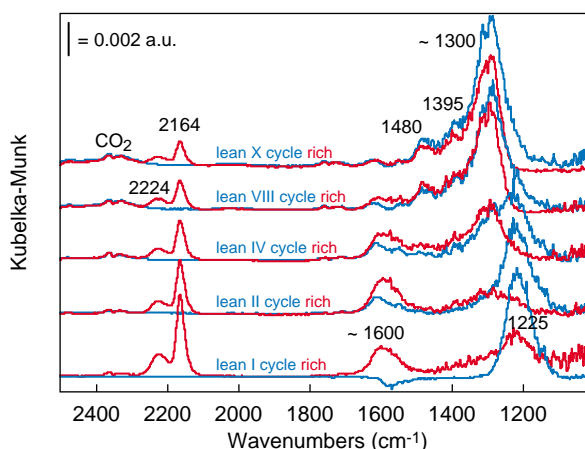

Figure 35

Ba/Al$_2$O$_3$ DRIFT spectra of the surface during 1 h of richness switchovers (lean phase (blue); rich phase (red)) at 723 K (spectra in common scale).

would require a gas chromatography or mass spectrometry analysis to check the presence of nitrogen in the exit gases. CO_2 (band at 2350 cm^{-1}) is present in larger quantities, an indication of the combustion of propylene.

The corresponding gas phase spectra again display no major differences to those discussed in the first test at 573 K *(Fig. 32)*. Hence they provide little additional data. The CO_2 band is apparently slightly more intense, but is difficult to quantify.

From these few richness switchover tests, a number of general conclusions can be drawn. As observed in the simple nitration tests, at low temperature nitrites are formed on the catalyst surface. Ba/Al$_2$O$_3$ traps the NO_x. At high temperature, part of the nitrites is converted to nitrates and other species appear (probably carbonates or hydrogeno-carbonate). Finally at 723 K, organo-nitrate species appear to form under rich phase, and then disappear under lean mixture. This behavior suggests a partial reduction of NO_x via cyanate and isocyanate (DeNO$_x$ action) at higher temperature.

Case of Pt/Al$_2$O$_3$

The same richness switchover experiment was conducted on this catalyst. The sample placed in the DRIFT cell was subjected to ten successive cycles of richness switchover from lean phase (NO/O$_2$/Ar) to rich phase (C$_3$H$_6$/Ar) (3 min and 3 min) at the following temperatures: 423, 498, 573, 648 and 723 K. The spectra recorded in single beam were reprocessed with that of the catalyst "activated" for 2 h under O$_2$/Ar at 873 K and recorded at 423 K.

Figure 36 shows the DRIFT spectra of the most signifi-cant cycles of the test at 423 K. From the first cycle we observe the formation of specific bands which steadily increase in intensity during one hour of test. Between lean
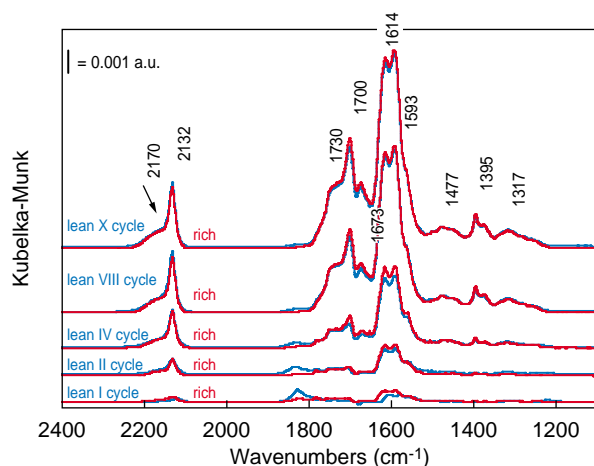
Figure 36

Pt/Al$_2$O$_3$ DRIFT spectra of the surface during 1 h of richness switchovers (lean phase (blue); rich phase (red)) at 423 K (spectra in common scale).

phase and rich phase there are no wide variations. We shall therefore merely discuss the final cycle. Compared with the simple nitration test, we observe the medium intensity band at 2132 cm^{-1} attributed to CO on oxidized Pt [38]. On the contrary, neither the isocyanate band on Al at 2222 cm^{-1} (AlNCO) [38], nor the NO band on Pt$^{\delta+}$ at 1836 cm^{-1}, nor the two nitrate bands at 1584 and 1548 cm^{-1}, are observed. Other bands appear. The shoulder at 2170 cm^{-1} can be attributed to an isocyanate on Pt (PtNCO) [34, 38]. The bands at 1700 and 1477 cm^{-1} suggest the presence of hydrogeno-carbonate (OCOOH) and those at 1593, 1395 and 1375 cm^{-1} suggest formiates (OCOH) on alumina [40]. The signal

at 1614 cm^{-1} is more difficult to attribute, but is probably due to the presence of water.

Figure 37 shows the DRIFT spectra pertaining to the tenth cycle (lean and rich phase) at rising temperature (423, 498, 573, 648 and 723 K). The attribution of the band at 1613 cm^{-1} to water appears to be confirmed in its disappearance at 498 K. At this temperature, the main species are still the hydrogeno-carbonates and formiates. The formiate bands are much more intense, indicating a predominance of these species. From 573 K on the contrary, different bands are observed. At 2156 cm^{-1} a wide medium-intensity band already attributed to the CN group on Al and at 1567 and 1466 cm^{-1} two intense bands of the carboxylate species of the acetate group (OCOCH$_3$) [39] are observed. The isocyanates, hydrogeno-carbonates and formiates are no longer observed. At higher temperature (648 K) the acetate bands begin to decrease in intensity and that of the AlCN increases to reach a maximum. The band at 1404 cm^{-1} cannot be attributed. At the maximum temperature (723 K) few species remain on the surface. (The band intensities are all sharply decreased and the surface is increasingly clean).

Some additional data are supplied by the analysis of the gas spectra leaving the DRIFTS cell *(Fig. 38)*, corresponding to the spectra of the surface already discussed. The quantity of CO$_2$ under rich phase increases with temperature, confirming that propylene and/or its oxidation products are consumed. Also observable from 573 K is the presence of CO in the gas phase (low intensity band at about 2150 cm^{-1}).

In conclusion, richness switchovers on a Pt/Al$_2$O$_3$ catalyst tend to promote the reduction of NO$_x$. The reaction mechanism often proposed in the literature suggests the initial reduction of NO by dissociation of the NO adsorbed on the Pt

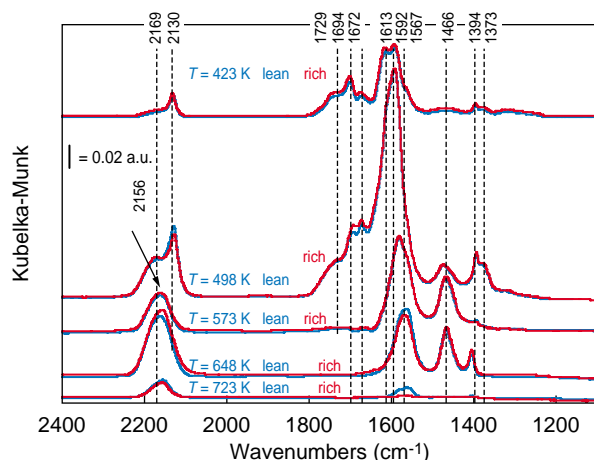Figure 37

Pt/Al$_2$O$_3$ DRIFT spectra of the surface during 1 h of richness switchovers (lean phase (blue); rich phase (red)) at different temperatures: Xth cycle (spectra in common scale).
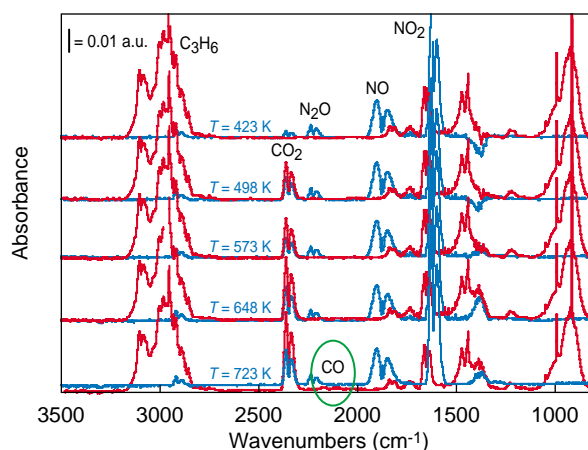

Figure 38

Pt/Al$_2$O$_3$ FT-IR spectra of the gas phase during 1 h of richness switchovers (lean phase (blue); rich phase (red)) at different temperatures: Xth cycle (spectra in common scale).

sites, followed by the combination of adsorbed N and NO to form N_2 or N_2O gas [41]. Propylene acts as a reducing agent in this context: by oxidizing to carboxylate and formiate, it releases the Pt sites of excess oxygen [41]. The results that we obtain confirm this mechanism, although analysis of the nitrogen leaving the DRIFTS cell and quantification of the products would be necessary to validate it. We can nonetheless state that the reduction of NO_x does not cause the formation of N_2O, as suggested in the mechanism reported above, because no increase in the intensity of the corresponding band is observed in the gas phase spectra *(Fig. 38)*.

CONCLUSIONS

These examples illustrate the broad range of data provided by the DRIFTS. We started with the simplest system, namely the recording of powder spectra at ambient temperature, which was complicated to permit temperature tracking with the recording of *in situ* spectra under inert or reaction atmosphere. We thereby investigated various types of catalysts, zeolites, boehmites and modified aluminas. The main advantages of this technique reside in the ease of sample preparation and the ability to analyze nontransparent materials, which could not be analyzed by transmission infrared spectroscopy. Besides, since the spectra are recorded *in situ*, one can "see" the catalyst working by monitoring the changes of species on its surface. The infrared spectroscopy analysis of the gases leaving the DRIFTS cell provides additional data: the gas mixtures can obviously be adapted according to the reaction investigated.

The information that can be obtained by diffuse reflection infrared spectroscopy remains qualitative, because the technique does not allow high quality quantitative measurements. However, a number of methods can be considered for quantitative analysis of the gases leaving the DRIFTS cell: gas chromatography if permitted by the type and quantity of the gases to be analyzed, or even mass spectrometry.

The technique could also permit analyses not only at atmospheric pressure but also under several tens of bar, suggesting the use of DRIFTS spectroscopy as a tool for characterization designed for work on catalysts in conditions very similar to those encountered during a catalytic action.

REFERENCES

1 *Industrial Analysis with Vibrational Spectroscopy* (1976) Calmers, J.M. and Dent, G. ed., The Royal Society of Chemistry, Cambridge.

2 Kubelka, P. and Munk, F. (1931) *Z. Tech. Phys.*, **12**, 593; Kubelka, P. (1948) *J. Opt. Soc. Am.*, **38**, 448.

3 Hamadeh, I.M. King, D. and Griffiths, P.R. (1984) Heatable-Evacuable Cell and Optical System for Diffuse Reflectance FT-IR Spectrometry of Adsorbed Species. *J. Catal.*, **88**, 264-272.

4 *The Infrared Spectra Handbook of Inorganic Compounds* (1984) Sadtler Research Laboratories, Division of Bio-Rad Laboratories Inc., Philadelphia (Pennsylvania-USA).

5 Jacobs, P.A. and Mortier, W.J. (1982) An Attempt to Rationalize Stretching Frequencies of Lattice Hydroxyl Groups in Hydrogen Zeolites. *Zeolites*, **2**, 226-230.

6 Barthomeuf, D. (1977) *Molecular Sieves II*, ACS Symp. 40, Am. Chem. Soc., Washington, DC, 453.

7 Ward, J.W. (1976) *Zeolite Chemistry and Catalysis*, ACS Monograph 171 (Ed. J.A. Rabo) Am. Chem. Soc., Washington, DC, 118.

8 Liu, X., Truitt, R.E. and Hodge, G.D. (1998) DRIFTS Studies of Surface Properties of Steamed FCC Catalysts. *J. of Catal.*, **176**, 52-60.

9 Nortier, P., Fourre, P., Mohammed Saad, A.B., Saur, O. and Lavalley, J.C. (1990) Effects of Crystallinity and Morphology on the Surface Properties of Alumina. *Applied Catal.*, **61**, 141-160.

10 Armaroli, T., Minoux, D., Gautier, S. and Euzen, P. (2003) A DRIFTS Study of Mo/alumina Interaction: from Mo/boehmite Solution to $Mo/\gamma Al_2O_3$ Support. *Applied Catalysis A: General*, **251**, 241–253.

11 Ewing, F.J. (1935) *J. Chem. Phys.*, **3**, 420.

12 Magela de Aguilar Cruz, A. and Guillaume Eon, J. (1998) Boehmite-Supported Vanadium Oxide Catalysts. *Applied Catal A: General*, **167**, 203-213.

13 Raybaud, P., Digne, M., Iftimie, R., Wellens, W., Euzen, P. and Toulhoat, H. (2001) Morphology and Surface Properties of Boehmite (gamma-ALOOH): a Density Functional Study. *J. Catal.*, **201**, 236-246.

14 Morterra, C., Emanuel, C., Cerrato, G. and Magnacca, G. (1992) Infrared Study of Some Surface Properties of Boehmite (γ-AlO$_2$H). *J. Chem. Soc. Faraday Trans.*, **88**, 339-348.

15 Fransen, T., Van der Meer, O. and Mars, P. (1976) Investigation of Surface Structure and Activity of Molybdenum Oxide Containing Catalysts. Infrared Study if Surface Structure of Molybdena-Alumina Catalysts. *J. Catal.*, **42**, 79-86.

16 Ratnasamy, P. and Knözinger, H. (1978) Infrared and Optical Spectroscopic Study of Co-Mo-Al$_2$O$_3$ Catalysts. *J. Catal.*, **54**, 155-165.

17 Topsøe, N.Y. (1980) Infrared Study of Sulfided Co-Mo-Al$_2$O$_3$ Catalysts. The Nature of Surface Hydroxyl Groups. *J. Catal.*, **64**, 235-237.

18 Okamoto, Y. and Imanaka, T. (1988) Interaction Chemistry between Molybdena and Alumina - Infared Studies of Surface Hydroxyl Groups and Adsorbed Carbon Dioxide on Aluminas Modified with Molybdate, Sulfate or Fluorine Anions. *J. Phys. Chem.*, **92**, 7102-7112.

19 Topsøe, N.Y. and Topsøe, H. (1993) FTIR Studies of Mo/Al$_2$O$_3$ Based Catalysts. Morphology and Structure of Calcined and Sulfided Catalysts. *J. Catal.*, **139**, 631-640.

20 Botto, L., Garcia, A.C. and Thomas, H.J. (1992) Spectroscopical Approach to Some Heteropolymolybdates with the Anderson Structure. *J. Chem. Solids*, **53**, 8, 1075-1080.

21 Minoux, D. (2002) Préparation de catalyseurs d'hydrotraitement par comalaxage molybdène/boehmite : influence sur les propriétés texturales, structurales et catalytiques du matériau final. *PhD Thesis*, University of P. et M. Curie (Paris VI).

22 Payen, E., Grimblot, J. and Kasztelan, S. (1987) Study of Oxidic and Reduced Alumina Supported Molybdate and Heptamolybdate Species by *in situ* Laser Raman Spectroscopy. *J. Phys. Chem.*, **91**, 6642-6648.

23 Knözinger, H. and Jeziorowski, H. (1978) Raman Spectra of Molybdenum Oxide Supported on Surface of Aluminas. *J. Phys. Chem.*, **82**, 2002-2005.

24 Carrier, X., Lambert, J.F. and Che, M. (1997) Ligand-Promoted Alumina Dissolution in the Preparation of MoOx/γ-Al$_2$O$_3$ Catalysts: Evidence for the Formation and Deposition of an Anderson-Type Alumino Hetero-Polymolybdate. *J. Amer. Chem. Soc.*, **119**, 42, 10137-10146.

25 Le Bihan, L., Blanchard, P., Fournier, M., Grimblot, J. and Payen, E. (1998) Raman Spectroscopic Evidence for the Existence of 6-Molybdoaluminate Entities on an Mo/Al$_2$O$_3$ Oxidic Precursor. *J. Chem. Soc., Faraday Trans*, **94**, 7, 937-940.

26 Fitzgerald, J.J., Piedra, G., Dec, S.F., Seger, M. and Maciel, G.E. (1997) Dehydration Studies of a High Surface Area Alumina (Pseudo-Boehmite) Using Solid State H[1] and Al[27] NMR. *J. Amer. Chem. Soc.*, **119**, 7832-7842.

27 Minoux, D., Diehl, F., Euzen, P., Jolivet, J.P. and Payen, E. (2002) A New Insight into Molybdtate/Boehmite Interaction. *Stud. Surf. Sci. Catal.*, **143**, 767-775.

28 Tsukada, T., Segawa, H., Yasumori, A. and Okada, K. (1999) Crystallinity of Bohemite and its Effetc on the Phase Transition Temperature of Alumina. *J. Mater. Chem.*, **9**, 549-553.

29 Busca, G., Lorenzelli, V., Ramis, G. and Willey, R. (1993) Surface Sites on Spinel-Type and Corundum-Type Metal Oxide Powders. *Langmuir*, **9**, 1492-1499.

30 Peri, J.B. (1982) Computerized Infrared Studies of Mo/Al$_2$O$_3$ and Mo/SiO$_2$ Catalysts. *J. Phys. Chem.*, **86**, 1615-1622.

31 Digne, M., Sautet, P., Raybaud, P., Euzen, P. and Toulhoat H. (2002) Hydroxyl Groups on γ-alumina Surfaces: a DFT Study. *J. of Catal.*, **211**, 1-5.

32 Morterra, C. and Magnacca, G. (1996) A Case Study: Surface Chemistry and Surface Structure of Catalytic Aluminas, as Studied by Vibrational Spectroscopy of Adsorbed Species. *Catal. Today*, 27, 497-532.

33 Srinivasan, S., Narayanan, C.R. and Datye, A.K. (1995) The Role of Sodium and Structure on the Catalytic Behavior of Alumina. IR spectroscopy. *Appl. Catal.*, **132**, 289-308.

34 Freysz, J.L. (2002) Réduction catalytique sélective des oxydes d'azote par le propène en excès d'oxygène sur platine supporté. *PhD Thesis*, Univ. Caen.

35 Ghorbel, A. and Primet, M. (1976) *J. Chim. Phys.*, **73**, 89.

36 Morrow, B.A., McFarlane, R.A. and Moran, L.E. (1985) Infrared Study of the Reaction between NO and O$_2$ and of the Adsorption of NO$_2$ on platinum. *J. Phys. Chem.*, **89**, 77-80.

37 Levoguer, C.L. and Nix, R.M. (1996) A Study of the Adsorption of NO on a Polycrystalline Pt Foil by FT-RAIRS. *Surf. Sci.*, **365**, 672-682.

38 Meunier, F.C., Breen, J.P., Zuzaniuk, V. and Ross, J.R.H. (1999) Mechanistic Aspects of the Selective Reduction of NO by Propene over Alumina and Silver-Alumina Catalysts. *J. Catal.*, **187**, 493-505.

39 Meunier, F.C., Zuzaniuk, V., Breen, J.P., Olsson, M. and Ross, J.R.H. (2000) Mechanistic Differences in the Selective Reduction of NO by Propene over Cobalt- and Silver-Promoted Alumina Catalysts: Kinetic and *in situ* DRIFTS Study. *Catalysis Today*, **59**, 287-307.

40 Busca, G., Lamotte, J., Lavalley, J.C. and Lorenzelli, V. (1987) FT-IR Study of the Adsorption and Transformation of Formaldehyde on Oxide Surfaces. *J. Am. Chem. Soc.*, **109**, 5197-5202.

41 Burch, R., Sullivan, J.A. and Watling, T.C. (1998) Mach-Anistic Considerations for the Reduction of NOx over Pt/Al$_2$O$_3$ and Al$_2$O$_3$ Catalysts under Lean-Burn Conditions. *Catalysis Today*, 42, 13-23.

Final manuscript received in January 2004